อนุภาคนาโนของอนุพันธ์ไคโทซานสำหรับการปลดปล่อยแบบควบคุมของแอลดีไฮด์

นาย ฐาปกรณ์ ตรีอุดม

วิทยานิพนธ์นี้เป็นส่วนหนึ่งของการศึกษาตามหลักสูตรปริญญาวิทยาศาสตรมหาบัณฑิต
สาขาวิชาปิโตรเคมีและวิทยาศาสตร์พอลิเมอร์
คณะวิทยาศาสตร์ จุฬาลงกรณ์มหาวิทยาลัย
ปีการศึกษา 2553

CHITOSAN DERIVATIVE NANOPARTICLES FOR CONTROLLED RELEASE OF ALDEHYDES

Mr. Thapakorn Tree-udom

A Thesis Submitted in Partial Fulfillment of the Requirements
for the Degree of Master of Science Program in Petrochemistry and Polymer Science
Faculty of Science
Chulalongkorn University
Academic Year 2010

Thesis title	CHITOSAN DERIVATIVE NANOPARTICLES FOR CONTROLLED RELEASE OF ALDEHYDES
By	Mr. Thapakorn Tree-udom
Field of Study	Petrochemistry and Polymer Science
Thesis Advisor	Associate Professor Supason Wanichwecharungruang, Ph.D.

Accepted by the Faculty of Science, Chulalongkorn University in Partial Fulfillment of the Requirements for the Master's Degree

…….Dean of the Faculty of Science
(Professor Supot Hannongbua, Dr.rer.nat.)

THESIS COMMITEE

.....Chairman
(Associate Professor Supawan Tantayanon, Ph.D.)

.....Thesis Advisor
(Associate Professor Supason Wanichwecharungruang, Ph.D.)

…….Examiner
(Associate Professor Nuanphun Chantarasiri, Ph.D.)

……..…External Examiner
(Panya Sunintaboon, Ph.D.)

ฐาปกรณ์ ตรีอุดม : อนุภาคนาโนของอนุพันธ์ไคโทซานสำหรับการปลดปล่อยแบบควบคุมของแอลดีไฮด์ (CHITOSAN DERIVATIVE NANOPARTICLES FOR CONTROLLED RELEASE OF ALDEHYDES) อ. ที่ปรึกษาวิทยานิพนธ์หลัก: รศ.ดร.ศุภศร วนิชเวชา รุ่งเรือง, 73 หน้า

งานวิจัยนี้สามารถเตรียมระบบควบคุมการปลดปล่อยที่มีสองชั้นประกอบด้วย ชั้นของพอลิเมอร์ผ่านอนุพันธ์ของไคโทซาน (ซัคซินิลไคโทซาน) และชั้นของพันธะเคมีผ่านอนุพันธ์ของแอลดีไฮด์ (ชิฟเบส) ภายใต้ปฏิกิริยาวิวิธพันธ์ ทำการสังเคราะห์ซัคซินิลไคโทซานโดยอาศัยปฏิกิริยาของไคโทซานกับซัคซินิคแอนไฮไดรด์ ซึ่งพอลิเมอร์ที่ได้สามารถเกิดการรวมตัวเป็นอนุภาคระดับนาโนในน้ำ โดยอนุภาคที่ได้สามารถสร้างพันธะชิฟเบสระหว่างหมู่อะมิโนบนพื้นผิวของอนุภาคของซัคซินิลไคโทซานกับแอลดีไฮด์ที่ให้กลิ่น ได้แก่ วานิลลิน ซินนามาลดีไฮด์ ซิโทรเนลลาล และซิทรอล ซึ่งพันธะชิฟเบสจะอยู่ภายในอนุภาคจากการยืนยันตำแหน่งโดยเทคนิคเอ็กซเรย์โฟโตอิเล็กตรอน อนุภาคนาโนชิฟเบสทั้ง 4 ชนิด มีความเสถียรและมีขนาดเส้นผ่านศูนย์กลางในช่วง 80 ถึง 165 นาโนเมตร ระบบนี้แสดงให้เห็นถึงการปลดปล่อยแอลดีไฮด์ที่ยาวนานขึ้นได้

สาขาวิชา ปิโตรเคมีและวิทยาศาสตร์พอลิเมอร์ ลายมือชื่อนิสิต……...……...……...

ปีการศึกษา……2553……......ลายมือชื่อ อ.ที่ปรึกษาวิทยานิพนธ์หลัก…...…...……..

5172272723: MAJOR PETROCHEMISTRY AND POLYMER SCIENCE
KEYWORDS: CHITOSAN/ N-SUCCINYLCHITOSAN/ SCHIFF BASE/ CONTROLLED RELEASE

THAPAKORN TREE-UDOM: CHITOSAN DERIVATIVE NANOPARTICLES FOR CONTROLLED RELEASE OF ALDEHYDES. THESIS ADVISOR: ASSOC. PROF. SUPASON WANICHWECHARUNGRUANG, Ph.D., 73 pp.

This research was able to prepare double barrier controlled release system consisting of a polymeric barrier through chitosan's derivation (*N*-succinylchitosan) and a chemical barrier through aldehyde's derivation (Schiff base) under heterogeneous phase reaction. *N*-succinylchitosan was synthesized based on the reaction of chitosan with succinic anhydride, and the obtained polymer could self-assemble into spherical nanoparticles in aqueous medium. The amino groups on the surface of the obtained particles could form Schiff base with fragrant aldehydes including vanillin, cinnamaldehyde, citronellal and citral. All the Schiff base moieties were located at the inside of the particles as confirmed by X-ray photoelectron spectroscopic analysis (XPS). All obtained Schiff base nanoparticles gave stable nanospheres, whose hydrodynamic diameters were in the range of 80 to 165 nm. The prolonged release of the grafted aldehydes from the obtained double barrier systems was demonstrated.

Field of Study: Petrochemistry and Polymer Science Student's Signature…….
Academic Year: ……2010……..... Advisor's Signature……

ACKNOWLEDGEMENTS

First of all, I would like to express my sincere appreciation to my thesis advisor, Associate Professor Dr. Supason Wanichwecharungruang for her helpful supervision, invaluable assistance and generous encouragement to fulfill my achievement.

I also sincerely thank Associate Professor Dr. Supawan Tantayanon, Associate Professor Dr. Nuanphan Chantarasiri and Dr. Panya Sunintaboon for their time and suggestions as the committee members.

I would not forget to thank the Development and Promotion of Science and Technology talents project (DPST), National Center of Excellence for Petroleum, Petrochemicals and Advanced Materials (NCE-PPAM) and Graduate School, Chulalongkorn University for scholarship and financial support. Very grateful thanks are extended to Professor Masayuki Yamaguchi and Mr. Murakami Tatsuya, School of Material Science, Japan Advanced Institute of Science and Technology, Japan for the XPS analysis and Associate Professor Dr. Sanong Ekgasit for ATR-FTIR analysis.

Last but not least, I would like to specially thank my family and my friends especially in Dr. Supason's Lab for their advice and encouragement throughout my master study.

CONTENTS

Page

ABSTRACT IN THAI……..... iv

ABSTRACT IN ENGLISH…..……..... v

ACKNOWLEDGEMENTS…..…….….. vi

LIST OF TABLES……..... x

LIST OF FIGURES……..…….... xi

LIST OF SCHEMES ……..……...…. xv

LIST OF ABBREVIATIONS……..... xvi

CHAPTER I: INTRODUCTION…….…….... 1

1.1 Fragrance aldehyde molecules ……..... 4

- Vanillin…….…. 4

- Cinnamaldehyde…….……. 5

- Citronellal……...…..… 5

- Citral…….…… 6

1.2 Derivatives of fragrance aldehyde molecules ……..…....… 6

- Schiff base formation ……..…..……... 7

- α-Acetoxy ethers formation…… 7

- Reversible hydrazone formation ……..... 8

- Acid-labile acetal formation ……..... 8

1.3 Formation of Schiff base……..…….. 9

1.4 Carrier in fragrance delivery system …….……...…. 10

- Use of chitosan…… 10

- Use of cyclodextrin……. 11

- Use of mesoporous silica…….… 12

- Use of homo- and copolymers……..…….…. 13

- Use of polymerblend…….….. 14

1.5 Chitosan…….…. 15

1.6 Carrier from chemical modification of chitosan…….….... 16

- Chitosan-poly(acrylic acid) nanoparticles……..… 16

- *N*-phthaloylchitosan-grafted mPEG nanospheres……. 17

Page

- Chitosan-*g*-poly(n-butyl acrylate) particles……..…….. 17
- *N*-succinyl-chitosan nanospheres……... 18
1.7 Research goals……..... 18
CHAPTER II: EXPERIMENTAL……..... 20
2.1 Materials and Chemicals……..…….…….. 20
2.2 Preparation of *N*-succinylchitosan (N-SCS)…….. 20
2.3 Nanoparticle formation……...…… 21
- Steady-state fluorescence spectroscopy……. 22
2.4 Preparation of imine-chitosan….……..... 22
2.5 Preparation of imine-N-SCS nanoparticles …… 23
- Optimization condition of reaction time during imine formation……..…..... 23
- Finding the optimum ratio between N-SCS nanoparticles and aldehyde……..…….. 24
- Various aldehydes for imine-N-SCS nanoparticles formation…….. 24
- Morphology, Hydrodynamic diameter and Zeta potential of the nanoparticles…….. 25
- Steady-state fluorescence spectroscopy…….. 25
- Chemical composition at the surface…….…….. 25
2.6 The release of aldehyde from Schiff base nanoparticles…...…. 26
- UV-visible spectroscopic analysis…….. 26
CHAPTER III: RESULTS AND DISCUSSION……..... 28
3.1 Preparation and characterization of *N*-succinylchitosan…… 28
3.2 Self-assembly of N-SCS……. 31
3.3 Preparation of imine-chitosan……. 33
3.4 Preparation of imine-N-SCS nanoparticles……...… 34
- Optimization condition of reaction time during imine formation…….……..… 34
- Finding the optimum ratio between N-SCS nanoparticles and aldehyde……..…….. 35

Page

- Various aldehydes for imine-N-SCS nanoparticles formation…….. 35
- Morphology, Hydrodynamic diameter and Zeta potential of the nanoparticles…….. 40
3.5 Micelle forming behavior…… 44
3.6 Chemical composition at the surface……...…… 45
- Chitosan…… 46
- Self-assembled N-SCS spheres…… 46
- Non-self-assembled *N*-vanillidenechitosan……..….... 46
- Self-assembled *N*,*N*′-vanillidene-succinylchitosan……..… 46
3.7 The release of aldehyde from Schiff base nanoparticles...…… 48
- UV/Vis spectroscopic analysis……...……. 48
CHAPTER IV: CONCLUSION…….…... 52
REFFERENCES……... 53
APPENDIX ……..… 58
VITAE……... 73

LIST OF TABLES

Table **Page**

3.1 Schiff base products from four perfumery aldehydes……. 43

LIST OF FIGURES

Figure		Page
1.1	Example of cyclic acetal of carbohydrate...……	2
1.2	The mechanism of Norrish type II photooxidation …….....	2
1.3	Example of α-keto ester …….	3
1.4	Example of oxidative labile fragrance ……..……..	3
1.5	Dendritic material for enzyme-triggered release of alcohol…….....	3
1.6	Hydrolysis of β-keto ester to release of fragrance alcohol …….	4
1.7	Chemical structure of vanillin…….....	5
1.8	Chemical structure of cinnamaldehyde …….…….....	5
1.9	Chemical structure of citronellal ……..……..……..…	6
1.10	Chemical structure of citral …….……...	6
1.11	Monomeric (left) and polymeric Schiff bases (right). The amounts of aldehyde isolated are shown in brackets ……...…….....	7
1.12	Preparation of α-acetoxy ethers …….....	8
1.13	Reversible hydrazone formation ……...…….....	8
1.14	Synthesis of amphiphilic copolymer having acid-labile acetal in the side chain ……..…….....	9
1.15	Schiff base formation …….…….....	9
1.16	The mechanism of Schiff base formation …….....	10
1.17	Time course of oil release from microcapsules at various temperatures....	11
1.18	Fragrance release from gel formulation with uncomplexed fragrance (J) and gel formulation with complexed fragrance (JC) of (L) linalool (left) and (B) benzyl acetate (right)……..……..……..…	12
1.19	TGA curves of pure perfume, perfume–SiO_2 and polyelectrolyte-encapsulating perfume–SiO_2…….…….....	13
1.20	Release profiles at 55 ^{O}C of a pure DMPBA miniemulsion, 30 wt% DMPBA in nanocapsules and 50 wt% DMPBA in nanocapsules…..…….	14
1.21	Release profiles of the encapsulated fragrance by e-nose…….....	15
1.22	Deacetylation reaction of chitin……..	16
1.23	TEM micrograph of CS-PAA nanoparticles at pH 4.5……....	16

Figure **Page**

1.24 TEM and SEM micrographs of *N*-phthaloylchitosan-grafted mPEG nanospheres……. 17

1.25 TEM micrographs of PBA-chitosan particles……. 17

1.26 TEM micrographs of NSCS nanospheres……... 18

3.1 The picture of N-SCS products obtained at the mole ratios of succinic anhydride: chitosan of (a) 0.1:1 (N-SCS1) and (b) 0.2:1 (N-SCS2)……... 29

3.2 ^{1}H NMR spectrum of N-SCS2…… 29

3.3 ATR-FTIR spectra of (a) chitosan and (b) N-SCS2…… 30

3.4 The 1 mg/mL colloidal dispersion concentrations of (a) N-SCS1 and (b) N-SCS2…….. 30

3.5 X-ray powder diffraction patterns of (a) chitosan and (b) N-SCS2…… 31

3.6 SEM photographs of N-SCS2 nanoparticles at polymer concentration of 1000 ppm (a) at 20,000xmagnification and (b) at 50,000xmagnification.. 32

3.7 TEM photograph of N-SCS2 nanoparticles at polymer concentration of 1000 ppm…… 32

3.8 Size distributions of N-SCS2 nanoparticles……... 33

3.9 ATR-FTIR spectrum of *N*-vanillidenechitosan……. 34

3.10 ATR-FTIR spectra of *N,N′*-vanillidene-succinylchitosan studies on imine formation at various reaction times of (a) 0, (b) 4, (c) 8 and (d) 25 h……. 37

3.11 ATR-FTIR spectra of *N,N′*-vanillidene-succinylchitosan studies on imine formation at N-SCS: vanillin weight ratio of (a) 1:1, (b) 2:1, (c) 3:1, (d) 4:1 and (e) 5:1……..... 38

3.12 ATR-FTIR spectra of (a) N-SCS and (b) *N,N′*-vanillidene-succinyl chitosan prepared at N-SCS: vanillin weight ratio of 3:1, reaction time for 4h……...… 38

3.13 ATR-FTIR spectra of (a) N-SCS and (b) *N,N′*-cinnamylidene-succinyl chitosan prepared at N-SCS: cinnamaldehyde weight ratio of 3:1, reaction time for 4h……..... 39

Figure **Page**

3.14 ATR-FTIR spectra of (a) N-SCS and (b) *N*,*N*′-citronellalidene-succinyl chitosan prepared at N-SCS: citronellal weight ratio of 3:1, reaction time for 4h…….. 39

3.15 ATR-FTIR spectra of (a) N-SCS and (b) *N*,*N*′-citralidene-succinyl chitosan prepared at N-SCS: citral weight ratio of 3:1, reaction time for 4h…….…..… 40

3.16 SEM photographs of *N*,*N*′-vanillidene-succinylchitosan nanospheres at polymer concentration of 3000 ppm (a) at 20,000xmagnification and (b) at 50,000xmagnification……..…….. 41

3.17 AFM images of *N*,*N*′-vanillidene-succinylchitosan……... 41

3.18 AFM images of *N*,*N*′-cinnamylidene-succinylchitosan……. 42

3.19 AFM images of *N*,*N*′-citronellalidene-succinylchitosan…… 42

3.20 AFM images of *N*,*N*′-citralidene-succinylchitosan…… 43

3.21 Change of intensity ratio (I_{372}/I_{384}) versus concentration of polymers (a) N-SCS and (b) *N*,*N*′-citronellalidene-succinylchitosan…… 45

3.22 XPS high resolusion spectra of (a) chitosan, (b) self-assembled N-SCS spheres, (c) non-self-assembled *N*-vanilidenechitosan and (d) self-assembled *N*,*N*′-vanillidene-succinylchitosan spheres…….. 47

3.23 Time versus amount of vanillin remained from Schiff base nanospheres compared with free vanillin…….……. 49

3.24 Time versus amount of cinnamaldehyde remained from Schiff base nanospheres compared with free cinnamaldehyde…….…….. 49

3.25 Time versus amount of citronellal remained from Schiff base nanospheres compared with free citronellal…….. 50

3.26 Time versus amount of citral remained from Schiff base nanospheres compared with free citral……..…. 50

A1 ^{1}H NMR spectrum of *N*-succinylchitosan2 (N-SCS2)…… 59

A2 ATR-FTIR spectrum of chitosan……. 60

A3 ATR-FTIR spectrum of *N*-succinylchitosan (N-SCS)…… 60

A4 ATR-FTIR spectrum of *N*-vanillidenechitosan…….. 61

Figure **Page**

A5 ATR-FTIR spectrum of *N,N'*-vanillidene-succinylchitosan…….. 61

A6 ATR-FTIR spectrum of *N,N'*-cinnamylidene-succinylchitosan…… 62

A7 ATR-FTIR spectrum of *N,N'*-citronellalidene-succinylchitosan……..... 62

A8 ATR-FTIR spectrum of *N,N'*-citralidene-succinylchitosan……... 63

A9 Calibration curve of vanillin at 269 nm……..…. 63

A10 Calibration curve of cinnamaldehyde at 279 nm…… 64

A11 Calibration curve of citronellal at 231 nm…….. 65

A12 Calibration curve of citral at 232 nm……..… 66

LIST OF SCHEMES

Scheme		Page
2.1	Preparation of *N*-succinylchitosan …….	20
2.2	Preparation of imine-chitosan ……..…….....…….	22
2.3	Preparation of imine-N-SCS nanoparticles …….....	23
3.1	Preparation of *N*-succinylchitosan …….....……...	28
3.2	Preparation of *N*-vanillidenechitosan ……...……..…	33
3.3	Preparation of imine-N-SCS …….....	34
3.4	Preparation of *N*,*N*′-vanillidene-succinylchitosan…….....	35
3.5	Preparation of *N*,*N*′-cinnamylidene-succinylchitosan …….……..	36
3.6	Preparation of *N*,*N*′-citronellalidene-succinylchitosan …….…..…	36
3.7	Preparation of *N*,*N*′-citralidene-succinylchitosan ……..…	36

LIST OF ABBREVIATIONS

δ	chemical shift
°C	degree Celsius
DG	degree of grafting
DS	degree of substitution
g	gram (s)
Hz	hertz
h	hour
IR	Infrared
µg	microgram (s)
mg	milligram (s)
mL	milliliter (s)
mV	millivolt
mW	milliwatt
min	minute (s)
MW	molecular weight
nm	nanometer (s)
NMR	nuclear magnetic resonance
ppm	parts per million
%	percent
cm^{-1}	per centimeter (s)
SEM	Scanning electron microscope
N-SCS	*N*-succinylchitosan
TEM	Transmission electron microscope
UV	ultraviolet
cm^{-1}	unit of wavenumber (IR)
λ	wavelength

CHAPTER I
INTRODUCTION

Natural and synthetic volatile fragrance molecules have been used as perfume in a broad variety of everyday products, e.g., softeners, detergents, shower creams and deodorants, of which pleasantness of the odor and longevity of fragrances are the main consumer concerns. Fragrance chemical can be categorized according to their chemical functionalities into alcohols, esters, lactone, ethers, ketones, terpenes, and aldehydes. Amongst these the most unstable functionality is aldehyde. Odorous aldehydes although are popularly used in everyday products, they often lose their odor due to both their volatility and their reactive nature which leads to reaction with other components during product storage or usage. Volatility and reactivity of other groups of fragrance chemicals such as terpenes, were also a serious problem. Therefore it has become one of the main issues in the fragrance technology to inherit slow release and maintain a fragrance chemical stability [1].

Controlled release has been defined as a manner that active agents or ingredients are allowed to be available at a require site and time with a specific rate [2]. Up to now, the controlled fragrance release technology can be divided into two groups [3]: (1) Physical Encapsulation, fragrance molecules are encapsulated into well designed polymer to prolong the longevity and increase stability of the active molecules. Other benefits of encapsulation include ease of production, enhanced safety and expanded application in fragrance fields whereas the release behaviors depended on fragrances loading and capability of molecules to diffusion out which was controlled by vapor pressure and fragrance molecules-polymer matrix interaction [4, 5]; (2) Chemical Derivation, fragrance molecules are covalently bonded with suitable moieties through appropriated chemical bonds and thus becoming inactive, however, upon breaking of such bonds the fragrance molecules re-emerge. The fragrance derivatives in this strategy are usually called pro-fragrances [6, 7]. The chemical linkages or chemical bonds used in pro-fragrance must be breakable under desired condition in order to release the fragrance molecules under the intended circumstances (environmental trigger) when the product is being used. Examples of

the feasible environmental triggers include temperature, light, oxidation, enzymes, pH as well as water content.

Temperature

The general approach to break the covalent bond was heating. Several situations in everyday life condition like ironing, hair drying and cooking are available for bond breaking. For example, release of vanillin from cyclic acetal of carbohydrate (Figure 1.1) by thermal activation above 70 ^{o}C has been used in cooking [8].

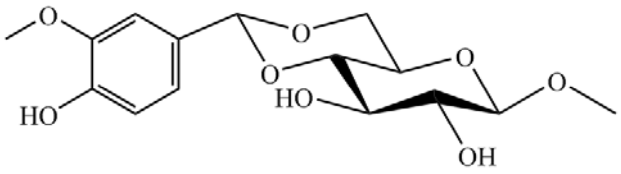

Figure 1.1 Example of cyclic acetal of carbohydrate

Light

Ultraviolet region, green natural energy from sunlight, is a source that can be used for covalent bond breaking. UV has been applied in the field of fragrance surface coating of which the fragrance molecules are triggered to be released from the surface upon an exposure to daylight [9]. Photooxidation of keto-ester is one of the Norrish type II reactions that could be employed to generate a good yield of aldehyde or ketone and carboxylic acid under outdoor sunlight in the presence of oxygen (Figure 1.2). Figure 1.3 showed cycloalkyl-oxo acetates as a photo-labile precursor for releasing of citronellal molecule [10].

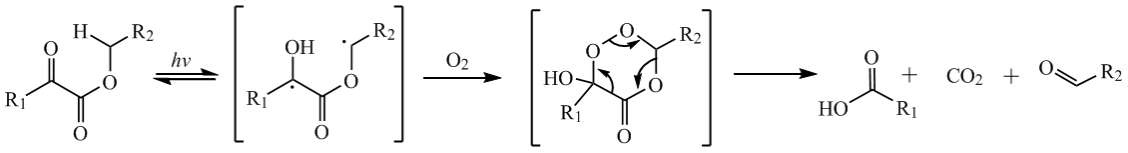

Figure 1.2 The mechanism of Norrish type II photooxidation

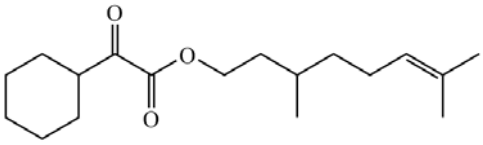

Figure 1.3 Example of α-keto ester

Oxidation

As it has been known that oxygen is active species which will easily react with various functional chemicals through oxidation reaction. Therefore, oxidation reaction has also been used to release fragrance chemicals from their pre-cursor molecules. In Figure 1.4, β-amino alcohol represents pro-fragrance precursor which by slow oxidation when exposed to the air could release aldehyde [11].

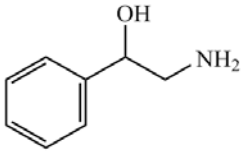

Figure 1.4 Example of oxidative labile fragrance

Enzymes

An interesting approach for breaking the designed labile fragrance molecules is the use of enzymes or antibacteria. Lipase is the useful enzyme found in the extracellular *Stratum corneum* of the skin [12] and also in skin bacteria [13] and it was used to trigger the release of fragrance. For example, the release of citronellol by lipase from dendritic substrate composed of branched polyamides conjugated to fragrance alcohol through ester bond (Figure 1.5) [14].

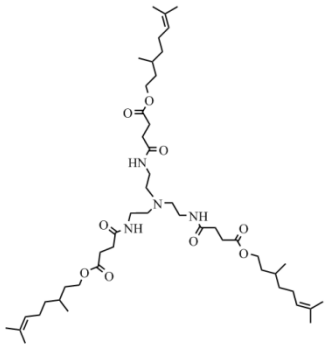

Figure 1.5 Dendritic material for enzyme-triggered release of alcohol

Hydrolysis and change in pH

Most personal care products are usually formulated in water base, therefore, it is logical to use hydrolytic labile pro-fragrance to control the release of fragrance molecules in order to increase fragrance longevity of the products. In some cases, hydrolysis may be affected by changing in pH value. Anderson and Fráter [15] reported a slow release of alcohol from β-keto ester through an ester hydrolysis with decarboxylation under acid- base conditions (Figure 1.6).

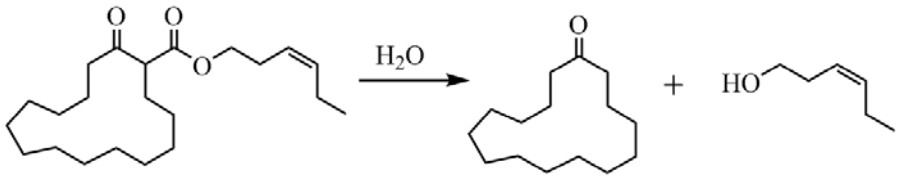

Figure 1.6 Hydrolysis of β-keto ester to release of fragrance alcohol

1.1 Fragrance aldehyde molecules

Fragrance molecules are either volatile organic compound isolated from plants and other natural sources or products from modern organic synthesis. They are generally used as ingredients in perfumes. Their odorous characteristics can be categorized into three notes: (1) top note, consisting of a small molecule that quickly evaporate to give a fresh, floral or fruity odor (2) middle note, consisting of less volatile substantive that give the scent before top note dissipation (3) base note, consisting of heavy-molecular weight molecule that slowly evaporate to give a deep odor [16].

Aldehydes represent a large percentage of odorous materials. Thus controlling the release of aldehydes will definitely benefits directly to the perfumery industry. In this works, selected aldehydes including both aliphatic and aromatic, were being used. The detail of each fragrance aldehydes is as follows.

Vanillin

Vanillin, 4-hydroxy-3-methoxybenzaldehyde ($C_8H_8O_3$), is a phenolic aldehyde compound which is a white solid appearance with the molecular weight of 152.15 g/mol. This compound contains aldehyde, ether and phenol functional group (Figure

1.7). Vanillin is partially soluble in water but well soluble in ethanol and methanol. It can be obtained from natural extraction and chemical synthesis. Natural vanillin is extracted from seed pods of vanilla. Synthetic vanillin is synthesized in two steps from guaiacol and glyoxylic acid precursor. Vanillin is usually used as an ingredient in foods, a flavoring additive in beverages and a key element in perfumes [17].

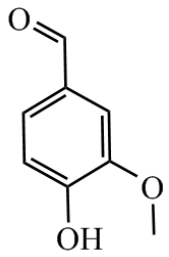

Figure 1.7 Chemical structure of vanillin

Cinnamaldehyde

Cinnamaldehyde, 3-phenylprop-2-enal (C_9H_8O), is an aromatic aldehyde compound which is a yellow oil appearance with the molecular weight of 132.16 g/mol. This compound contains phenyl group and unsaturated aldehyde (Figure 1.8). Cinnamaldehyde is slightly soluble in water but soluble in ethanol. It can be obtained from the steam-distillation process from the bark of cinnamon trees. Cinnamaldehyde is usually used as a flavoring additive in beverages and foods, and as a fragrance molecule to give a sweet or fruity scent in perfume. It is also well-known as an insecticide, an antioxidant, an anti-microbial and an anti-septic agent [18].

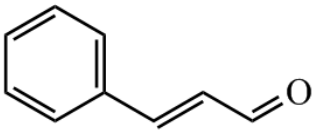

Figure 1.8 Chemical structure of cinnamaldehyde

Citronellal

Citronellal, 3,7-dimethyloct-6-en-1-al ($C_{10}H_{18}O$), is an aliphatic aldehyde compound (Figure 1.9) which is a clear to yellow oil appearance with the molecular weight of 154.25 g/mol. This compound is the major component of the citronella oil.

Citronellal is insoluble in water but soluble in ethanol, ether, chloroform and acetone. It can be isolated from the steam-distillation process of the leaves of different species of *Cymbopogon* grass. Citronellal is usually used as a mosquito repellent, and as a fragrance in cosmetic products such as soaps and other toiletries. The compound gives a lemon scent. It is also reported that the compound inherits some anti-fungal property [19].

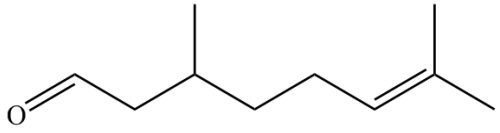

Figure 1.9 Chemical structure of citronellal

Citral

Citral, 3,7-dimethyl-2,6-octadienal ($C_{10}H_{16}O$), is an aliphatic aldehyde compound (Figure 1.10) which is a pale yellow oil appearance with the molecular weight of 152.24 g/mol. This compound is the major component in the lemongrass oil, verbena oil, lemon oil, nikkel oil, lime oil, ginger oil, and other plant essential oils. Citral is insoluble in water but soluble in ethanol. It is usually used both as a flavor, and as a fragrance that gives a strong lemon scent. Citral is also a raw material for the synthesis of retinol, ionone and methylionone. It also finds in application as an insect repellent with anti-microbial properties [20].

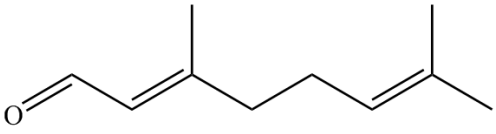

Figure 1.10 Chemical structure of citral

1.2 Derivatives of fragrance aldehyde molecules

Fragrances are highly volatile organic compounds thus their odorous perceptions are short-lived. As mentioned earlier that many of them, especially aldehydes, are unstable functional group that can undergo degradation prior to their

use in the products. To avoid these problems, pro-fragrances have been developed to prolong the fragrance release and stability. Pro-fragrances recently represent an attractive alternative way to conventional encapsulation techniques [7, 16]. They release one or several volatile compounds from well-designed precursor molecules through the cleavages of selective labile-covalent bond during product usage. Many labile chemical bonds have been designed for controlled release of their original molecules. The following paragraphs contain details of popular chemical functionalities used for this purpose.

Schiff base formation

In 1982, Kamogawa *et al*. [21] synthesized Schiff bases by reacting of *m*- or *p*-aminostyrenes with citral (an aldehyde) (Figure 1.11). The Schiff base products were obtained in ethanol without the use of high temperature. The *p*-Schiff bases showedhigher yields and higher melting points than the corresponding *m*-Schiff bases. For the hydrolysis of Schiff base products under acidic aqueous solution, it was found that the release rate of citral from the polymer was slower than that of the monomer. These demonstrated that the long-time release characteristic of fragrance molecules could be made possible when polymeric structure was applied.

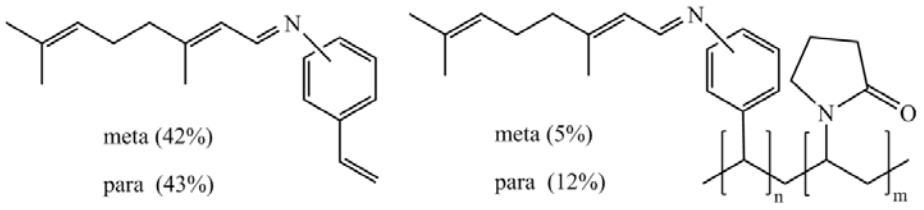

Figure 1.11 Monomeric (left) and polymeric Schiff bases (right). The amounts of aldehyde isolated are shown in brackets.

α-Acetoxy ethers formation

In 2005, Bochet and Robles [6] were able to prepare photolabile-aldehyde precursors through α-acetoxy ethers formation using the reduction reaction of the related esters with diisobutylaluminium hydride (DIBAL) and quenching aluminum

hemiacetal (an intermediate) with acetic anhydride (Figure 1.12). These precursors were able to release aldehyde molecules when being exposed to UV light (at 350 nm). This model can be further developed into external-responsive smart materials.

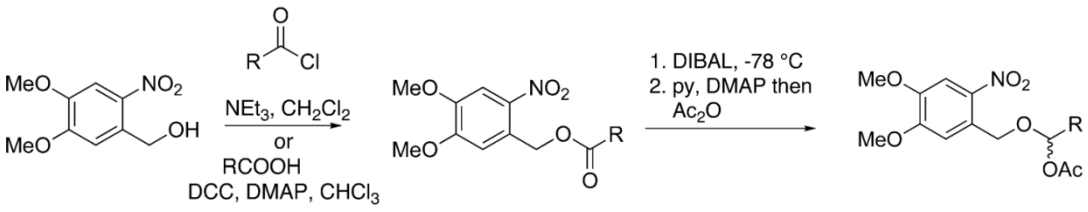

Figure 1.12 Preparation of α-acetoxy ethers

Reversible hydrazone formation

In 2006, Herrmann *et al*. [7] used the concept of reversible covalent reactions for the controlled delivery of volatile fragrance molecules. They demonstrated the reversible hydrazone formation through the reaction between hydrazine derivatives and aldehydes or ketones which had hemiaminal as an intermediate in a two-step mechanism (Figure 1.13). The gradual hydrolysis of the hydrazone makes it a highly efficient pro-fragrance material.

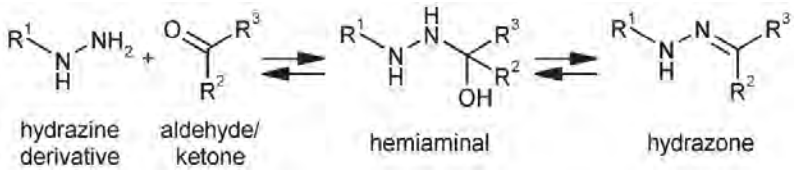

Figure 1.13 Reversible hydrazone formation

Acid-labile acetal formation

In 2009, Endo *et al*. [3] attached the volatile fragrance molecules into an amphiphilic copolymer through an acetal linkage by reacting of 2,3-dihydroxypropyl methacrylate monomer (diol) and lilial (aldehyde). Thus, a lilial-derived cyclic acetal attachment was synthesized (Figure 1.14). The obtained polymeric pro-fragrance possessed a very low vapor pressure of the fragrance molecule. Therefore, the rapid release of the fragrance molecules could be retarded.

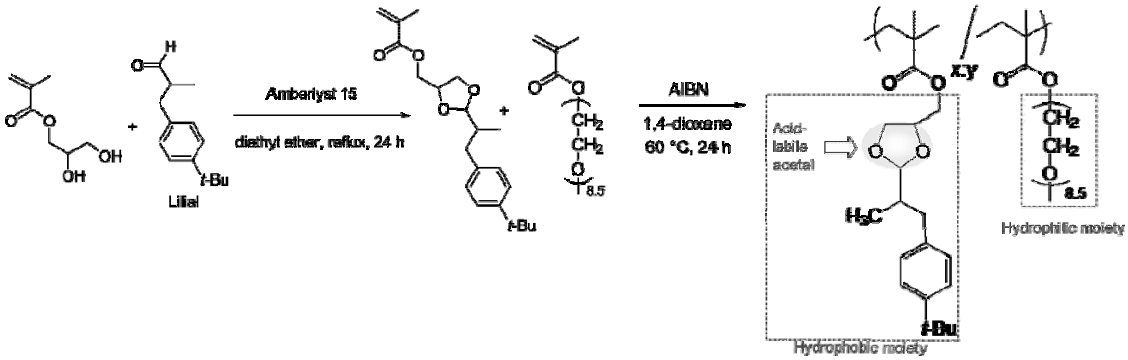

Figure 1.14 Synthesis of amphiphilic copolymer having acid-labile acetal in the side chain [3]

1.3 Formation of Schiff base

Amongst many chemical derivatization reactions of aldehyde, reactions of aldehydes with amino groups to form imine bonds or Schiff bases have been popularly used so far for the reason that Schiff base is tolerant under basic conditions but hydrolysable under acidic conditions, it is easy to control the release of the original molecules by changing the environmental pH. The imine product could be stored under dry condition and brought into water contact whenever the aldehyde release was required [16, 22]. Schiff base, a carbon-nitrogen double bond (C=N), could be obtained from the condensation reactions of amines and aldehydes/ketones. The Schiff base is nitrogen analogue of aldehyde or ketone with C=N in place of the carbonyl group (Figure 1.15).

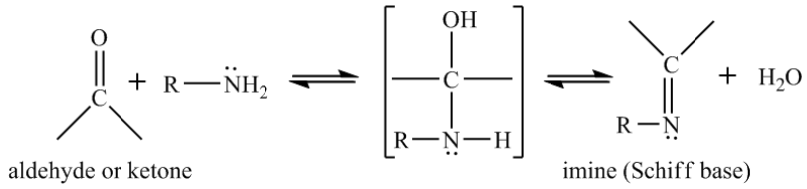

Figure 1.15 Schiff base formation

The mechanism of Schiff base formation starts with an acid-catalyzed nucleophilic addition of the amino group to carbonyl group, follow by deprotonation of nitrogen atom and finally loss of water to form a double bond [22] (Figure 1.16).

Step 1: Acid catalyzed addition of the amine to the carbonyl

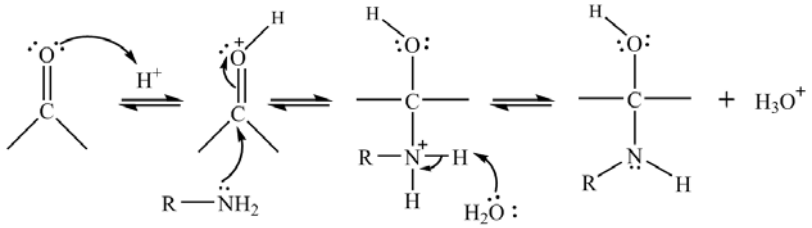

Step 2: Acid catalyzed dehydration

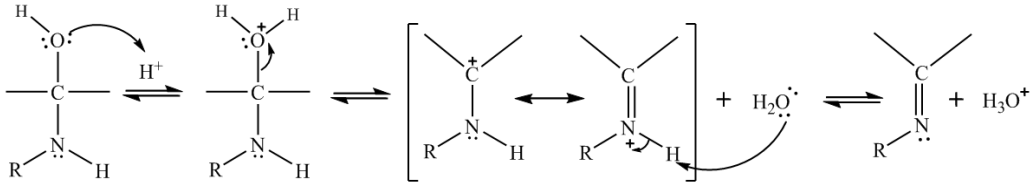

Figure 1.16 The mechanism of Schiff base formation

1.4 Carrier in fragrance delivery system

Poor solubility in water of many fragrances usually causes difficulty in product formulation. Although surfactant can be used as stabilizing agent, it is still faced with other problems such as turbidity, irritation and stability. The encapsulation of fragrance into carrier provides both increased solubility and controlled release characteristic. Through encapsulation technology, easy handling, increased safety and enhanced stability have also been realized. Herein, the recent carriers for long-time lasting fragrance release with different types of polymer are being reviewed.

Use of chitosan

In 2006, Wen *et al*. [23] prepared microcapsules for volatile essential oil encapsulation using oil-in-water (O/W) emulsion process, using chitosan as a wall material, citronella oil as an inner core material and coconut oil as a surfactant. The prepared sample at chitosan 0.5 wt%, NaOH 1.0 wt% with coconut oil possessed a good dispersion character and gave the encapsulation efficiency of 98.2%. The particle size of chitosan microcapsules decreased when the emulsification stirring rate increased. The release of citronella oil from the microcapsules was investigated by determining the time course of the microcapsules weight placed in an Infrared Moisture Determination Balance (IMDB). The release rate of citronella oil from

smaller microcapsules was faster than that of bigger microcapsules because of larger surface area. The release behaviors of the active after thermal pretreatment at 40 ^{o}C and 60 ^{o}C for 1 min were similar, whereas that at 80 ^{o}C was significantly slower. The author explained the slower release rate at high temperature through the closing of the pores induced by the wall shrinkage at high temperature (Figure 1.17).

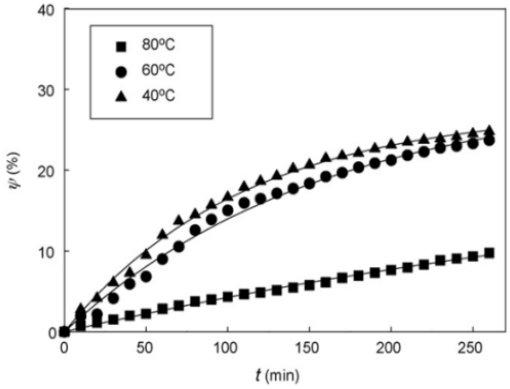

Figure 1.17 Time course of oil release from microcapsules at various temperatures [23]

Use of cyclodextrin

In 2007, Tarimci *et al*. [24] made the linalool and benzylacetate inclusion complexes using 2-hydroxypropyl-β-cyclodextrin (2-HPβCD) to improve the water solubility, stability, and control the release property of the two fragrance compounds. The inclusion complexes were confirmed using ^{1}H-NMR spectroscopy and circular dichroism spectroscopy. The results of the solubility experiments showed that the inclusion complex at molar ratio of guest:host of 1:1 increased the solubility for 5.9 4.2 folds for linalool and benzylacetate, respectively. The results of the 6-month-stability test showed less decrease of the fragrance concentration in the gel formulations with prepared inclusion complexes comparing to that with the uncomplexed fragrances. Furthermore, the results of the controlled release study showed slower fragrance released from the gel formulation with the inclusion complexes comparing to that with the uncomplexed fragrances (Figure 1.18).

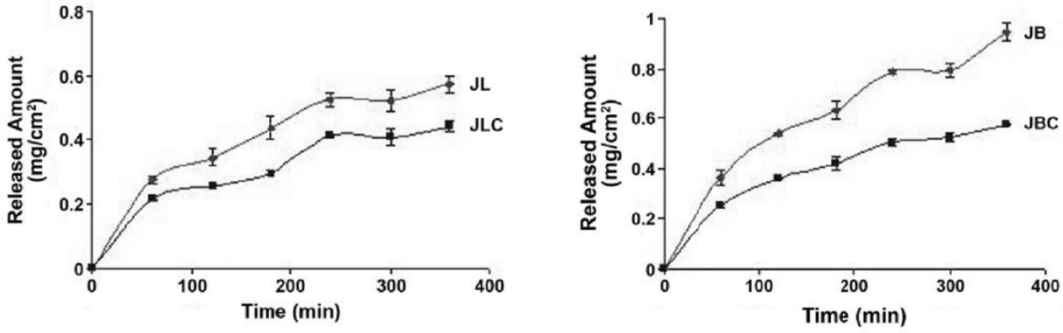

Figure 1.18 Fragrance release from gel formulation with uncomplexed fragrance (J) and gel formulation with complexed fragrance (JC) of (L) linalool (left) and (B) benzyl acetate (right) [24]

Use of mesoporous silica

In 2008, Wang *et al.* [25] successfully prepared perfume-encapsulating mesoporous silica spheres having polyelectrolyte shell for encapsulation of perfume. Mesoporous silica (MS) microspheres, having hydrophilic pore with large pore sizes and pore volumes, were used as supports for enlarge loading content of hydrophilic perfume. Ten layers of polyelectrolyte shell consisting of five layers of poly(diallyl dimethylammonium chloride) (PDDA) and five layers of poly(sodium 4-styrenesulphonate) (PSS) were alternately deposited by layer-by-layer on the obtained microspheres' surfaces through the interaction between positive charge of PDDA and negative charged of PSS in order to retard the release of perfume. The prolonged-release performances of composite microspheres were compared by thermogravimetric analysis (TGA) at 70 ^{o}C. The results of the experiment showed that almost all weight of free perfume quickly lose after 9 min, however the lifetime of perfume was increased after encapsulation and the weight could be retained up to 42% when the presence of polyelectrolyte shell (Figure 1.19). This indicated that the effective prolonged-release property of perfume results from the combination of the encapsulation of perfume into MS microspheres and the coating of the PDDA/PSS shells.

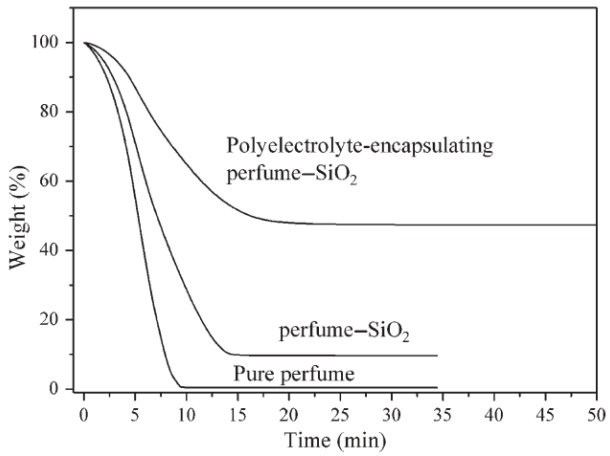

Figure 1.19 TGA curves of pure perfume, perfume–SiO_2 and polyelectrolyte-encapsulating perfume–SiO_2 [25]

Use of homo- and copolymers

In 2009, Landfester *et al.* [26] encapsulated the hydrophobic fragrance 1,2-dimethyl-1-phenyl-butyramide (DMPBA) into nanocapsules using one-step miniemulsion polymerization process. Polymeric shell of nanocapsules was fabricated with different types of homopolymers (poly(methylmethacrylate) (PMMA) and polystyrene (PS)) and copolymer (poly(methylmethacrylate-co-2-ethylhexyl methacrylate) P(MMA-co-2-EHA)). The different polymer shells possessed different glass transition temperatures (Tg). The release behaviors of the pure DMPBA and the encapsulated DMPBA at various fragrance contents were analyzed using ^{1}H NMR spectroscopy. At 20 ^{o}C below the Tg of polymer/fragrance, no release of fragrance was observed. The temperature of over 55 ^{o}C (T>Tg) caused significantly release of the fragrance (Figure 1.20). The results indicated that the release rate of the fragrance molecules can be easily controlled by changing capsule shell. In other words, the rate of fragrance release could be adjusted by selecting appropriated polymer shell of desired Tg.

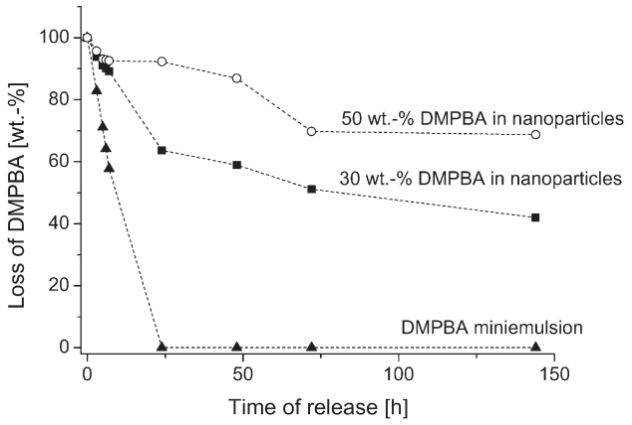

Figure 1.20 Release profiles at 55 ^{O}C of a pure DMPBA miniemulsion, 30 wt% DMPBA in nanocapsules and 50 wt% DMPBA in nanocapsules [26]

Use of polymer blend

In 2010, Sansukcharearnpon *et al*. [5] encapsulated the six fragrances, camphor, citronellal, eucalyptol, limonene, menthol and 4-tert-butylcyclohexyl into polymer blend based ethylcellulose (EC), hydroxypropylmethylcellulose (HPMC) and poly(vinylalcohol) (PV(OH)). The encapsulation process was carried out by solvent displacement method. This process gave nanospherical particles with the fragrance loading capacity and encapsulation efficiency of ≥40% and ≥80%, respectively, at weight ratio of the fragrance: polymer of 1:1. The release profiles of all encapsulated fragrances and pure fragrances were determined using thermogravimetric analysis (TGA) and electronic nose (e-nose). The results from both techniques were agreeably and it was concluded that the release of all tested fragrances except limonene could be prolonged by encapsulation into the polymer blend (Figure 1.21).

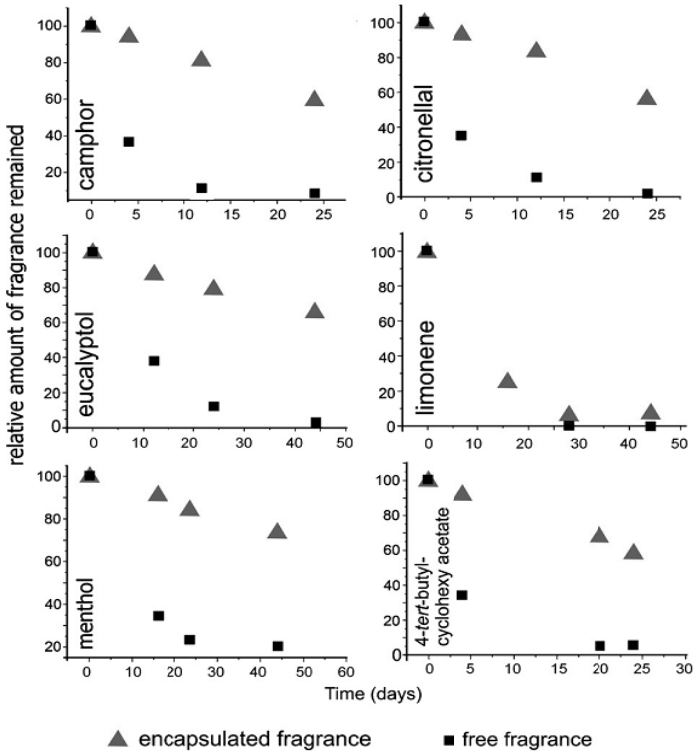

Figure 1.21 Release profiles of the encapsulated fragrance by e-nose [5]

1.5 Chitosan

Amongst many polymers, chitosan has been an interesting candidate for using as fragrance delivery host. Chitosan (β-(1→4)-2-amino-2-deoxy-β-D-glucan) is a biopolymer derived from chitin, naturally found in crustacean outer skin or fungal cell walls, by alkaline deacetylation reaction. To make chitosan, acetamide groups of chitin must be transformed into amino groups (Figure 1.22). Chitosan is used widely in many areas such as food, biotechnology, drugs and pharmaceuticals, materials science, and currently in gene therapy [23, 27-30]. Because the repeating units of chitosan consist of glucosamine (GlcN), N-acetylglucosamine (GlcNAc) units, chitosan possesses primary hydroxyl, secondary hydroxyl and amino groups, thus canafford several possibilities for chemical derivatization. Chitosan also possesses great properties such as biodegradability, biocompatibility, mucoadhesivity and anti-microbial activities [27-30].

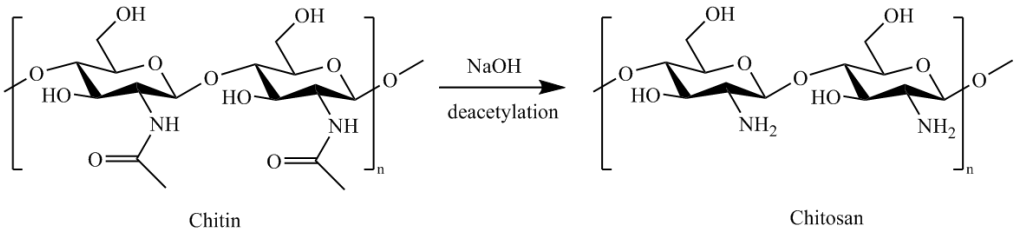

Figure 1.22 Deacetylation reaction of chitin

1.6 Carrier from chemical modification of chitosan

Although chitosan possesses many advantages, the compound is insoluble in almost all solvents except acids owing to its high compact-crystalline structure and high molecular weight. Consequently, many researchers have been working with chemically modified chitosan.

Chitosan-poly(acrylic acid) nanoparticles

In 2002, Yang *et al.* [31] prepared chitosan-poly(acrylic acid) complex nanoparticles (CS-PAA nanoparticles) using template polymerization. The polymerization of acrylic acid in chitosan solution (CS as the template) was initiated by $K_2S_2O_8$. After successful polymerization, the solution changed from a clear solution to an emulsion. The inter- and intra- molecular complexation between negative charge from carboxyl groups (COO^-) of PAA and positive charge from amino groups (NH_3^+) of CS leading to the formation of nanoparticles. The obtained particles, at pH 4.5 in aqueous solution, showed well dispersion and good particle stability, and possesses positive charge and small size in the range of 200 - 300 nm (Figure 1.23).

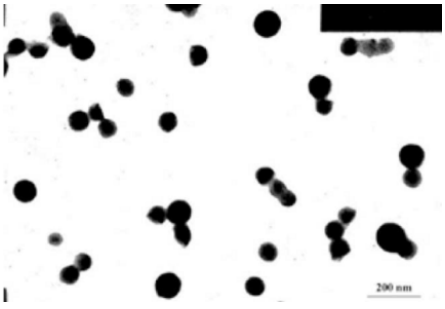

Figure 1.23 TEM micrograph of CS-PAA nanoparticles at pH 4.5 [31]

N-phthaloylchitosan-grafted mPEG nanospheres

In 2004, Yokson *et al*. [32] successfully produced *N*-phthaloylchitosan-grafted poly(ethylene glycol) methyl ether (mPEG) nanospheres by grafting mPEG-COOH (hydrophilic segment) onto the hydroxyl group of *N*-phthaloylchitosan. The grafted product displayed a turbid appearance when dispersed in water and other solvents. These colloidal phenomena indicating that the aggregated behavior of chitosan chains which was induced by the hydrophobic-hydrophilic interaction results in the sphere formation. The size of spheres was 80-100 nm (Figure 1.24).

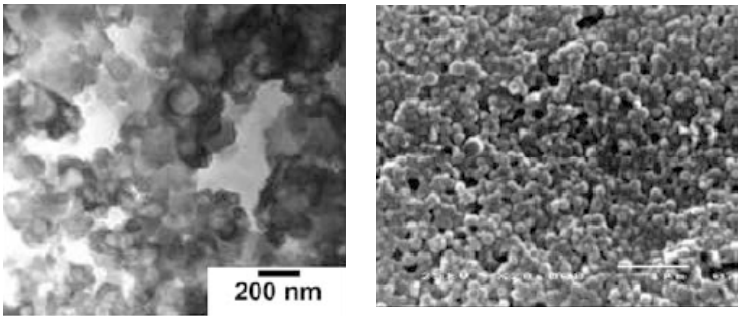

Figure 1.24 TEM and SEM micrographs of *N*-phthaloylchitosan-grafted mPEG nanospheres [32]

Chitosan-g-poly(n-butyl acrylate) particles

In 2005, Li *et al*. [33] synthesized a novel core-shell particles consisting of poly(n-butyl acrylate) (PBA) and chitosan by an emulsion copolymerization of BA in acidic chitosan solution with a small amount of *t*-butyl hydroperoxide. The core-shell structure of PBA-chitosan particles was well observed by transmission electron microscopy (TEM). TEM micrograph (Figure 1.25) could greatly define that the particle had a soft core PBA which was covered with a chitosan shell. In addition, the PBA-chitosan nanoparticles were positively charged with an average diameter of 300 nm.

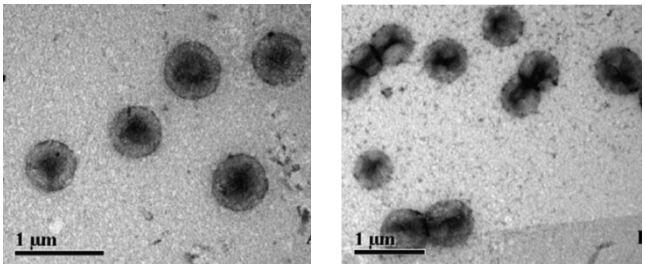

Figure 1.25 TEM micrographs of PBA-chitosan particles [33]

N-succinyl-chitosan nanospheres

In 2006, Zhu *et al*. [34] synthesized *N*-succinyl-chitosan nanospheres (NSCS), succinyl was substituted at hydrogen atom of amino group in chitosan chains. In distilled water, NSCS easily dispersed into the stable and transparent dispersion. Examining of the dispersion indicated an assembling of polymer into spherical particles. The self-assembly of the obtained nanospheres probably induce from the decrease in intermolecular H-bonding thus lower the crystallinity of the chitosan. The average size of the NSCS nanospheres was about 50–100 nm (Figure 1.26).

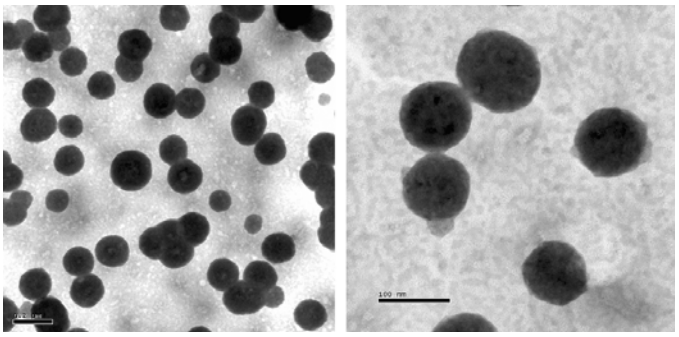

Figure 1.26 TEM micrographs of NSCS nanospheres [34]

1.7 Research goals

The aim of this research is to prepare the nanocarrier based biopolymer containing fragrance aldehyde molecules in order to effectively control the release of the fragrance aldehydes. The system consisted of succinylchitosan shell as a physical barrier and aldehyde linked to amine group of nanoparticles as a chemical barrier. The work included:

1. Preparation of *N*-succinylchitosan (N-SCS)
2. Preparation of fragrance aldehyde nanoparticles (imine-*N*-succinylchitosan nanoparticles)

- Preparation of *N*,*N*′-vanillidene-succinylchitosan
- Preparation of *N*,*N*′-cinnamylidene-succinylchitosan
- Preparation of *N*,*N*′-citronellalidene-succinylchitosan
- Preparation of *N*,*N*′-citralidene-succinylchitosan

3. Chemical structure, morphological observation and surface characterization of prepared nanoparticles

4. Controlled release study of imine-*N*-succinylchitosan nanoparticles compared with free fragrance aldehyde

CHAPTER II

EXPERIMENTAL

2.1 Materials and Chemicals

Chitosan powder with approximately 85% degree of deacetylation and 30,000 Da of viscosity-average molecular weight was purchased from Seafresh Chitosan (Lab) Co., Ltd (Bangkok, Thailand). Succinic anhydride, vanillin, citronellal and citral, chemicals analytical grade, were purchased from Acros organics (Geel, Belgium). Cinnamaldehyde was purchased from Aldrich (Steinheim, Germany). Other reagents were also analytical grade and were used without futher purification. Acetic acid, ethanol and acetone were purchased from Merck (Darmstadt, Germany).

2.2 Preparation of *N*-succinylchitosan (N-SCS)

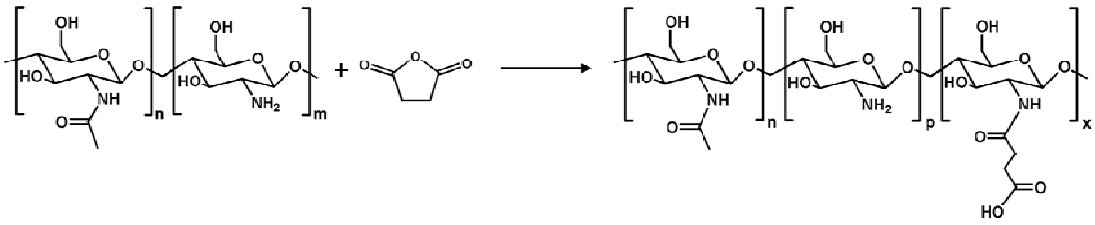

Scheme 2.1 Preparation of *N*-succinylchitosan

N-succinylchitosan (N-SCS) was prepared according Scheme 2.1. Succinic anhydride was allowed to react with each glucosamine unit of chitosan at mole ratios of 0.2:1 and 0.1:1. For each sample, 2.01 g of chitosan (12.5 mmole) was dissolved in 70 mL of 2%v/v acetic acid. The 0.25 and 0.125 g of succinic anhydride (2.50 and 1.25 mmoles, respectively) in 10 mL of acetone were slowly dropped into acidic chitosan solution while stirring, and the mixture was left at room temperature overnight. Then the reaction mixture was precipitated with excess acetone. The precipitate was collected by filtration and wash with acetone several times. Finally, a white powder was obtained. The product was characterized by Nuclear magnetic resonance (NMR), a Varian mercury spectrometer (Variance Inc., Palo Alto, USA),

operating at 400 MHz. Attenuated total reflectance-Fourier transform infrared (ATR-FTIR), a Continuμm^{TM} infrared microscope equipped with a mercury-cadmium-telluride (MCT) detector and connected to a Nicolet 6700 FT-IR spectrometer (Thermo Electron Corporation, Madison, WI, USA) and ATR accessory consisting of a slide-on miniature germanium (Ge) as the internal reflection element was used, collecting with 64 scans in the mid-infrared region (4000 – 650 cm^{-1}). X-ray diffraction (XRD), a Rigaku DMAX 2200/Ultima^{+} diffractometer (Rigaku International Corporation, Tokyo, Japan), using Cu Kα radiation operating at 40 kV and 30 mA and UV/Vis, a UV2500 spectrophotometer (Shimadzu Corporation, Kyoto, Japan), measuring in a quartz cell of pathlength 1 cm with thermostated at 25 ^{0}C, were also used during material characterization.

N-succinylchitosan (N-SCS): 75% yields of white powder and 0.18 degree of succinyl grafting. ^{1}H NMR (D_2O, 400 MHz, δ, ppm): 2.01 (H of acetyl groups), 2.42-2.50 (methylene protons of the succinyl), 2.80 (H2 of glucosamine, GlcN), 3.50-3.92 (H2′ of *N*-acetylglucosamine, GlcNAc, H3, H4, H5 and H6 of GlcNAc and GlcN), 4.54 (H1 of GlcNAc and GlcN). ATR-FTIR (cm^{-1}): 3282 (N-H stretching and O-H stretching vibration), 2864 (C-H stretching vibration), 1652 (amide I (C=O stretching)), 1555 (amide II), 1406 (symmetric stretching vibration of COO^{-} and amide III), 1319 (amide III (C-N stretching)), 1143 (C-O-C stretching vibration), and 1027 (C-O stretching vibration). UV/Vis (deionized water, 25^{o}C) λ max: 252 nm, ε: 0.0278 $M^{-1}cm^{-1}$(equivalent of monomeric unit).

2.3 Nanoparticle formation

Particles were simply prepared by dispersion of N-SCS (20 mg) into 20 mL deionized water thus the transparent colloid was obtained. Morphology of particles was visualized by scanning electron microscopy (SEM), a JSM-6400 (JEOL, Tokyo, Japan). A drop of nanoparticles dispersion was placed on a glass slide and dried overnight. The sample was coated with a gold layer under vacuum at 15kV for 90s then mounted on a SEM stud for visualization at an accelerating voltage of 15kV. A JEM-2100 transmission electron microscope (JEOL, Tokyo, Japan) was also acquired

for morphology studies. A drop of nanoparticles dispersion was placed onto carbon film coated on a copper grid and dried at room temperature. Observation was performed at 100-120 kV with 15 kV for accelerating voltage. Hydrodynamic diameter, polydispersity index (PDI) and zeta potential values were measured in deionized water by dynamic light scattering (DLS) technique using a Zetasizer nanoseries model S4700 (Malvern Instruments, Worcestershire, UK). Before measurement, the freshly prepared colloidal suspension was appropriately diluted, filtered with Millipore membrane filter (pore size: 0.45 µm) and ultrasonicated for five minutes. All measurements were repeated in triplicate and mean values were reported.

Steady-state fluorescence spectroscopy

One milliliters of pyrene solution ($1x10^{-5}$ M in methanol) was placed in a test tube and methanol was dried under nitrogen atmosphere. Ten mililiters of aqueous solution of N-SCS of various concentrations (0.05, 0.10, 0.15, 0.20, 0.25, 0.30, 0.35, 0.40, 0.45, 0.50, 0.55 and 0.60 mg/ml) was added into the test tube to obtained 1 µM final concentration of pyrene. Then the solution was kept at room temperature overnight for equilibration before subjected to spectrofluorometric analysis, a Varian Cary Eclipse spectrofluorometer, (Varian Optical Spectroscopy Instruments, Mulgrave, Victoria, Australia). The sample was excited at 334 nm, the emission was recorded from 350 to 450 nm and the fluorescent intensity at 372 and 384 nm were recorded.

2.4 Preparation of imine-chitosan

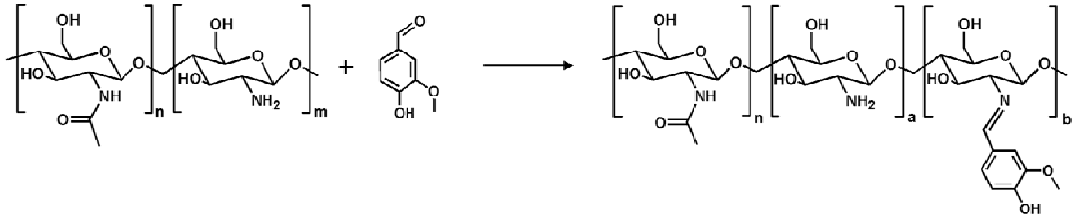

Scheme 2.2 Preparation of imine-chitosan

Sixty milligrams of chitosan was dissolved in 16 mL of 2% v/v acetic acid. Twenty milligrams of vanillin was dissolved in 4 mL of ethanol and then the solution was added drop-wise into acidic chitosan solution. The mixture was continuously stirred at room temperature for 4 h, then, a drop of the obtained product was placed on the glass slide and left to dry in vacuum desicator and the dry material was used for ATR-FTIR and XPS analysis.

N-vanillidenechitosan: ATR-FTIR (cm^{-1}): 3289 (N-H stretching and O-H stretching vibration), 2877 (C-H stretching vibration), 1635 (C=N stretching vibration), 1592 and 1512 (C=C stretching vibration of aromatic), 1150 (C-O-C stretching vibration), and 1027 (C-O stretching vibration).

2.5 Preparation of imine-N-SCS nanoparticles

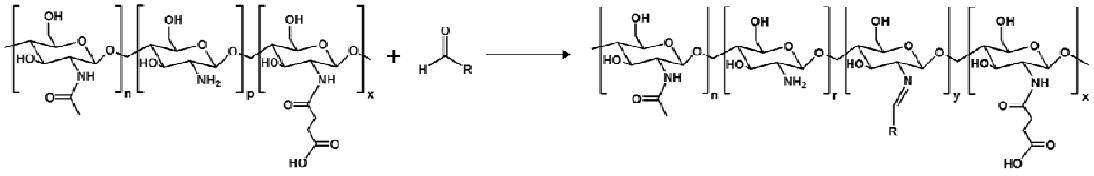

Scheme 2.3 Preparation of imine-N-SCS nanoparticles

Optimization condition of reaction time during imine formation

Imine-N-SCS nanoparticles (Schiff base's particles) were prepared by heterogeneous phase-grafting reaction. The suitable reaction time (reaction between amine group of N-SCS and the aldehyde functionality of vanillin as a representative aldehyde) was determined using the weight ratio of N-SCS powder: vanillin of 1:1. Sixty milligrams of N-SCS was dispersed in 16 mL deionized water. The alcoholic solution (60 mg of vanillin in 4 mL of ethanol) was slowly dropped into the aqueous phase under sonication (40 KHz, 30 ^{o}C) and then the mixture was futher sonicated for various times, i.e., 0, 4, 8 and 25 h. Aliquotes of the obtained product at various sonication times were immediately analyzed by ATR-FTIR after drying on the glass slide under vacuum.

Finding the optimum ratio between N-SCS nanoparticles and aldehyde

For finding the optimum ratio between aldehyde and amine (no unreacted aldehyde left after the reaction but with maximum Schiff base formation), the same procedure as describe above was used but with the 4 h sonication time. The amine in N-SCS nanoparticles was allowed to react with aldehyde in the vanillin structure at the weight ratio of N-SCS to vanillin of 1:1, 2:1, 3:1, 4:1 and 5:1. The imine bond formation was characterized through ATR-FTIR.

Various aldehydes for imine-N-SCS nanoparticles formation

In this experiment, both aliphatic and aromatic aldehydes were employed as perfumery aldehyde. Vanillin and cinnamaldehyde are representatives of aromatic aldehyde while citronellal and citral are representatives of aliphatic aldehyde. All the experiments were carried out under the optimal condition obtained from the above experiment (the weight ratio of polymer to aldehyde was 3:1 and sonication time of about 4h). Briefly, 20 mg of the aldehyde in 4 mL ethanol was added into the suspension of N-SCS (60 mg, 16 mL) under sonication environment, after 4h the product was left dry and then characterized through ATR-FTIR.

N,N'-vanillidene-succinylchitosan: Degree of vanillin substitution: 0.34. ATR-FTIR (cm^{-1}): 3282 (N-H stretching and O-H stretching vibration), 2867 (C-H stretching vibration), 1635 (C=N stretching vibration), 1592 and 1512 (C=C stretching vibration of aromatic), 1555 (amide II), 1143 (C-O-C stretching vibration), and 1027 (C-O stretching vibration).

N,N'-cinnamylidene-succinylchitosan: Degree of cinnamaldehyde substitution: 0.29. ATR-FTIR (cm^{-1}): 3282 (N-H stretching and O-H stretching vibration), 2867 (C-H stretching vibration), 1632 (C=N stretching vibration), 1592 (C=C stretching vibration of aromatic), 1552 (amide II), 1147 (C-O-C stretching vibration), and 1024 (C-O stretching vibration).

N,N'-citronellalidene-succinylchitosan: Degree of citronellal substitution: 0.38. ATR-FTIR (cm^{-1}): 3282 (N-H stretching and O-H stretching vibration), 2870 (C-H stretching vibration), 1638 (C=N stretching vibration), 1612 (C=C stretching

vibration), 1552 (amide II), 1147 (C-O-C stretching vibration), and 1024 (C-O stretching vibration).

N,N'-citralidene-succinylchitosan: Degree of citral substitution: 0.38. ATR-FTIR (cm^{-1}): 3282 (N-H stretching and O-H stretching vibration), 2874 (C-H stretching vibration), 1638 (C=N stretching vibration), 1612 (C=C stretching vibration), 1555 (amide II), 1143 (C-O-C stretching vibration), and 1027 (C-O stretching vibration).

Morphology, Hydrodynamic diameter and Zeta potential of the nanoparticles

The particle morphology of the products was observed using SEM, TEM and atomic force microscopy (AFM, a Nanoscope IV scanning probe microscope (Veeco Metrology Group, California, USA), operating in tapping mode). For the AFM analysis, before visualization, a drop of nanoparticles dispersion was placed on a glass slide and dried overnight. The average hydrodynamic diameter, polydispersity index (PDI) and zeta potential values of samples were conducted by dynamic light scattering (DLS).

Steady-state fluorescence spectroscopy

The emission spectra of the mixture between imine-N-SCS nanospheres (*N,N'*-citronellalidene-succinylchitosan nanospheres) of various concentrations and a fluorescence probe (pyrene at a selected concentration) were recorded on spectrofluorimeter. The measurement was carried out using the same procedure as described in N-SCS (λ_{excite} = 334 nm, the emission was recorded from 350 to 450 nm). The change in I_{372}/I_{384} as the intensities of pyrene at the first and the third peaks were used to determine the range of critical aggregation concentration (cac) value.

Chemical composition at the surface

Functional groups present on chitosan surface and surface of the fabricated nanospheres of the modified material (N-SCS, *N*-vanillidenechitosan, *N,N'*-vanillidene-succinylchitosan nanospheres) were obtained through X-ray photoelectron spectroscopy (XPS), a Kratos AXIS Ultra DLD instrument (Kratos, Manchester,

England), using a monochromatic Al Kα X-ray source (1486.6 eV). The X-ray source was operated at 150 W (15 kV and 10 mA). The base pressure in the XPS analysis chamber was about 5×10^{-8} torr during the measurement. All binding energies (BEs) were referenced to the hydrocarbon C 1s peak at 285 eV. High resolution spectra for the C1s and N1s were acquired using pass energy of 20 eV and energy steps of 0.1 eV. Data analysis was performed with the Kratos Vision Processing software.

2.6 The release of aldehyde from Schiff base nanoparticles

UV-visible spectroscopic analysis

Five milliliters of each Schiff base dispersion (*N,N′*-vanillidene-succinylchitosan, *N,N′*-cinnamylidene-succinylchitosan, *N,N′*-citronellalidene-succinylchitosan and *N,N′*-citralidene-succinylchitosan at polymer and aldehyde concentration of 7500 and 2500 ppm, respectively) was loaded in a 20 mL flat bottom headspace vial for 7 vials per each of the dispersion and all of the vials were left uncovered at 32 ^{o}C. When reach the 0, 1, 2, 5, 8, 12 and 16 days, the sample vial was adjusted volume to 10 mL by adding 20% v/v ethanol, changed to pH 1.0 with 1 M HCl, filled with 15 mL of hexane, and then immediately capped with headspace aluminum crimp caps with PTFE/silicone septa. The hexane layer was then subjected to aldehyde quantitation using a UV-visible spectrophotometer with the aid of a calibration curve of each standard aldehyde comparing with free perfumery aldehydes.

The release of perfumery aldehydes was also evaluated in dry samples at 40 ^{O}C. Here 10 ml of the freshly prepared imine-N-SCS nanoparticle suspensions (prepared at final concentration of aldehyde of 2500 ppm) were left in the uncapped 20 ml flat bottom-headspace-vial for 60 days. Under this condition the samples became dry after 20 days, as no water was added into the vials, and the dry samples were kept at the same condition until the 60-day period was reached. Control samples were solutions of corresponding aldehydes at 2500 ppm (in 20% (v/v) ethanol-water).

Then after 60 days, each sample vial was filled with 15 ml of 50% (v/v) ethanol-water, the sample was kept 24 h, and the ethanol-water phase was subjected to aldehyde quantification as described above.

CHAPTER III

RESULTS AND DISCUSSION

The amine functionality on the C2 of glucosamine unit of chitosan chain is highly nucleophilic and can easily react with acid anhydrides, ketones and aldehydes [35]. Therefore, it is quite popular to modify especially the amino group of chitosan chain with various chemical reactions to fabricate water-soluble chitosan derivatives. Recently, Aiping Zhu and coworkers [34] reported a simple process for preparing water-soluble non-toxic *N*-succinylchitosan, which can self-assembly in water to form nanosphere. Here we used the same reaction to obtain the *N*-succinylchitosan, which was subsequently modified into double barrier fragrant nanospheres.

3.1 Preparation and characterization of *N*-succinylchitosan

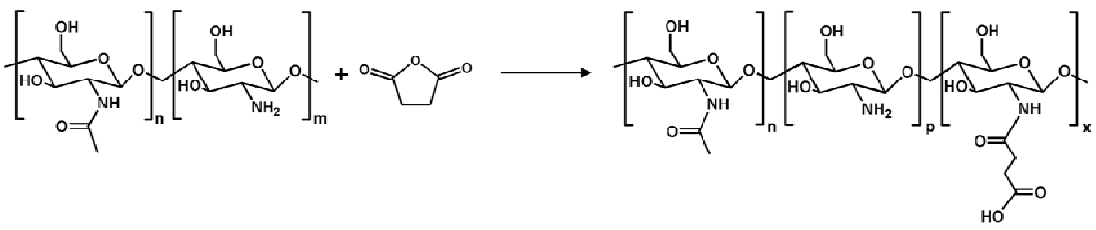

Scheme 3.1 Preparation of *N*-succinylchitosan

The reaction for derivatization of chitosan is present in Scheme 3.1. The chitosan derivative was prepared *via* a succinylation reaction between amino group and succinic anhydride to form *N*-succinylchitosan (N-SCS).

The physical appearance of the synthetic N-SCS obtained from reactions conducted at mole ratios between the succinic anhydride: amino group of the chitosan of 0.1:1 and 0.2:1 were pale yellow (N-SCS1) and white (N-SCS2) powder, respectively (Figure 3.1).

Figure 3.1 The picture of N-SCS products obtained at the mole ratios of succinic anhydride: chitosan of (a) 0.1:1 (N-SCS1) and (b) 0.2:1 (N-SCS2)

The successful succinyl moiety grafting was confirmed by NMR and ATR-FTIR. For ^{1}H NMR spectrum of N-SCS2 in D_2O (Figure 3.2), signal appearing at 2.42-2.50 ppm assigned to dimethylene protons of grafted succinyl was observed. Using the integral ratio between 4H from ethyl group of succinyl and 1H from C2 of glucosamine unit (at 2.8 ppm) with 85% deacetylation degree, the degree of grafting could be estimated as 0.18. ATR-FTIR spectrum (Figure 3.3) showed new absorption band at 1555 and 1406 cm^{-1} corresponding to N-H bending vibration of amide II and symmetric stretching vibration of COO^{-} and C-N stretching vibration of amide III, respectively.

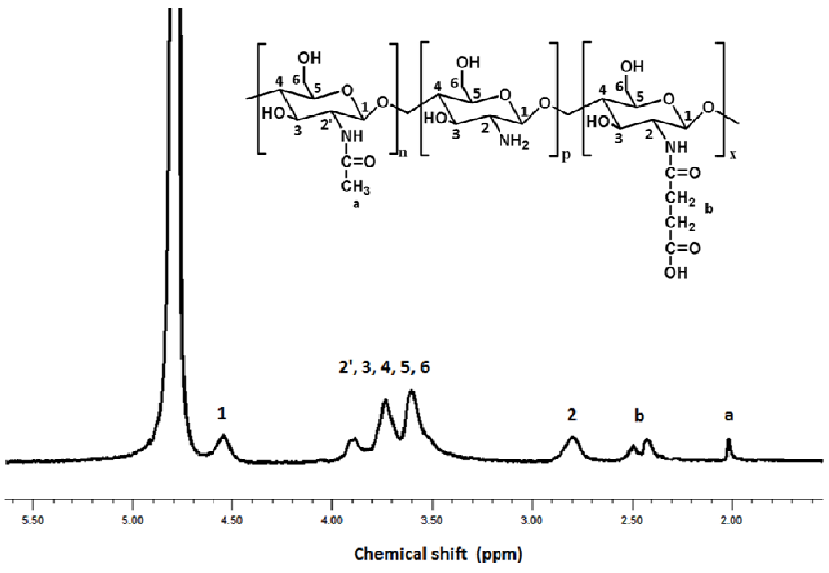

Figure 3.2 ^{1}H NMR spectrum of N-SCS2

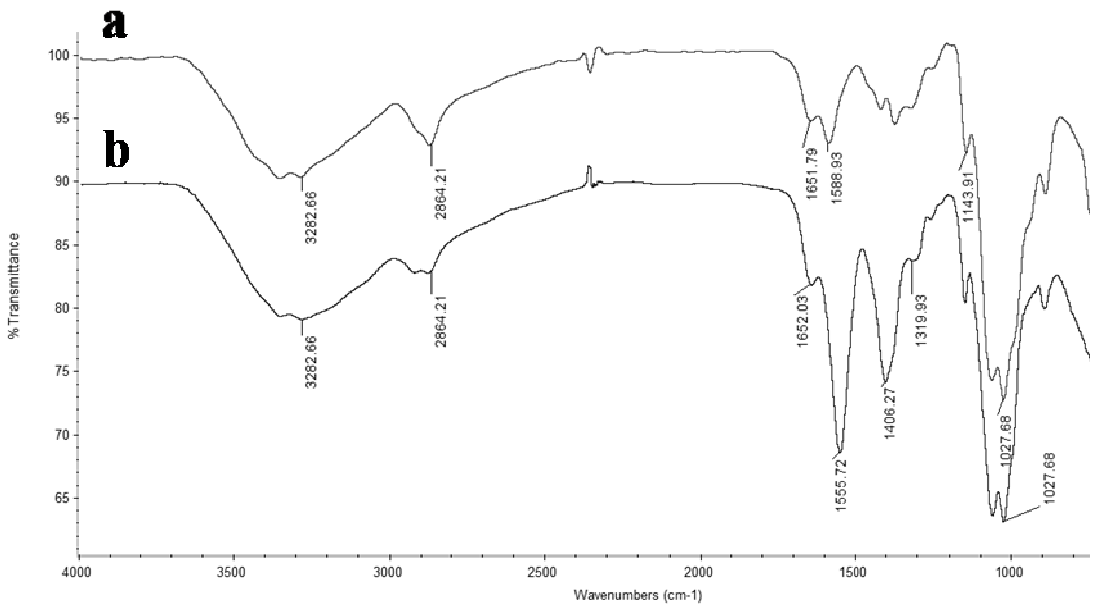

Figure 3.3 ATR-FTIR spectra of (a) chitosan and (b) N-SCS2

Since one of the main objectives to first prepare N-SCS was to overcome the water insolubility of chitosan, thus the water dispersibility of the product was seriously considered. And it was found that the N-SCS could disperse well in water. Inter/intramolecular hydrogen bonding of the obtained N-SCS should become less pronounced comparing to the original chitosan, thus N-SCS could easily disperse in deionized water and self-assembly to obtain the colloidal dispersion with stable and transparent features [34].

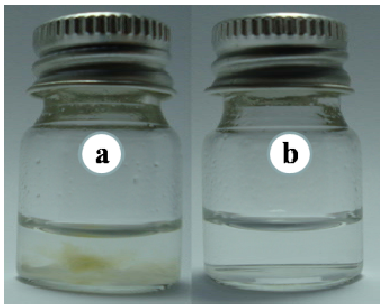

Figure 3.4 The 1 mg/mL colloidal dispersion concentrations of (a) N-SCS1 and (b) N-SCS2

Comparing between N-SCS1 and N-SCS2, a better transparent colloidal suspension in water was observed for N-SCS2 (Figure 3.4b). This result indicated that the dispersibility increased when the amount of succinyl group of N-SCS increasing.

The crystallographic structure of chitosan and the grafted polymer was determined using X-ray powder diffraction (XRD) analysis. The XRD diffractograms of chitosan exhibited peaks at 2θ of 11^o and 20^o [36] whereas only one broad peak at 2θ of 20^o was observed for N-SCS2 (Figure 3.5). The disappearance of the peak at 2θ of 11^o indicated decreased crystallization, changed polymer packing and destructed intermolecular hydrogen bonding.

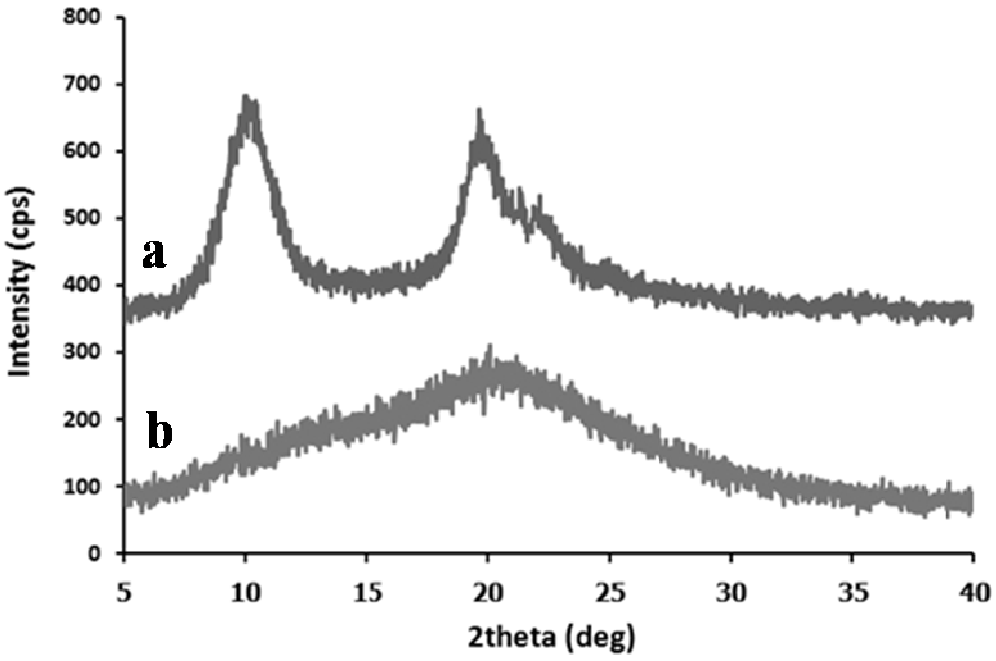

Figure 3.5 X-ray powder diffraction patterns of (a) chitosan and (b) N-SCS2

3.2 Self-assembly of N-SCS

Assembly behaviors of chitosan derivatives in aqueous medium based on electrostatic interactions, hydrophobic interactions and hydrogen bonding have been reported [37]. In the N-SCS structure, hydrophilic moieties include succinyl moieties, carboxylic, hydroxyl, amine and amide groups whereas ethyl ($-CH_2CH_2-$) and acetyl

groups and glucosidic ring constitute hydrophobic parts of the structure. In the N-SCS aqueous suspension, the inter/intramolecular association of hydrophobic groups and inter/intramolecular hydrogen bonding affect the particle formation. When the hydrophobic and hydrophilic parts along the N-SCS structure together with interaction with the medium (water in this case) are balanced, the N-SCS can self-assembly into stable particles.

The N-SCS in aqueous system showed transparent colloidal suspension. The suspension of the sample was left to dry before being subjected to SEM and TEM analysis. SEM photographs showed the regular spherical particles in nanoscale size (Figure 3.6). The nanoparticles were also confirmed by TEM (Figure 3.7).

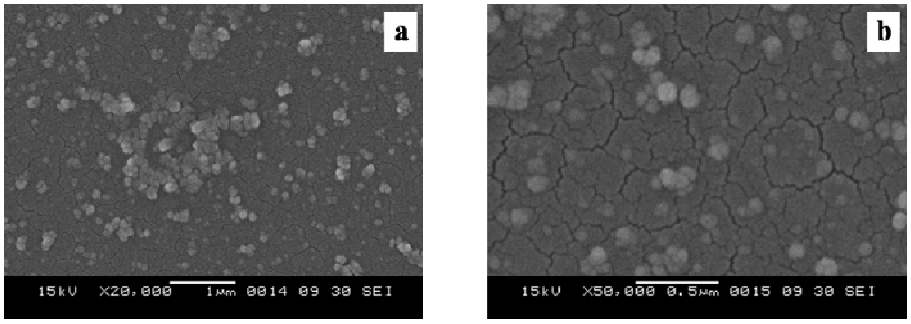

Figure 3.6 SEM photographs of N-SCS2 nanoparticles at polymer concentration of 1000 ppm (a) at 20,000xmagnification and (b) at 50,000xmagnification

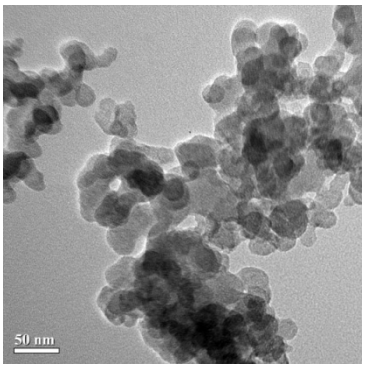

Figure 3.7 TEM photograph of N-SCS2 nanoparticles at polymer concentration of 1000 ppm

Dynamic light scattering (DLS) measurement of the freshly prepared suspension was carried out to obtain the hydrodynamic diameter, polydispersity index (PDI) and zeta potential value. The diluted N-SCS2 aqueous suspension gave a small hydrodynamic diameter (mean value±S.D.) of 46.3±0.24 nm with a narrow size distribution (PDI of 0.185). Figure 3.8 showed size distribution spectrum of N-SCS2 measured by DLS, supporting the particle diameter ranged from 10 to 130 nm and corresponding to average size of 46 nm. However, the size of the obtained particles was bigger than that observed by TEM. This indicated some swelling of the polymer-SCS particles when suspended in water. The mean zeta potential of N-SCS2 nanoparticles was positive value (22.3±2.6 mV) when measured at pH of around 5.5. Protonation of amine groups is speculated as the cause of the positive charge at the particle surface.

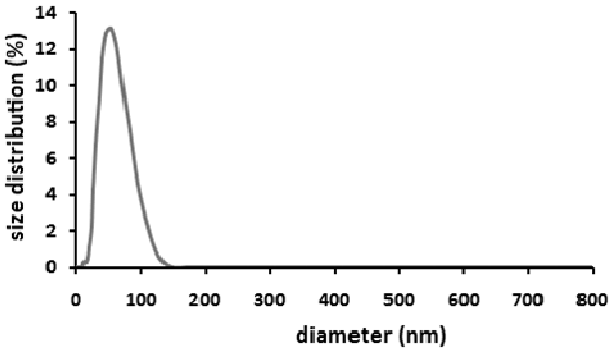

Figure 3.8 Size distribution of N-SCS2 nanoparticles

3.3 Preparation of imine-chitosan

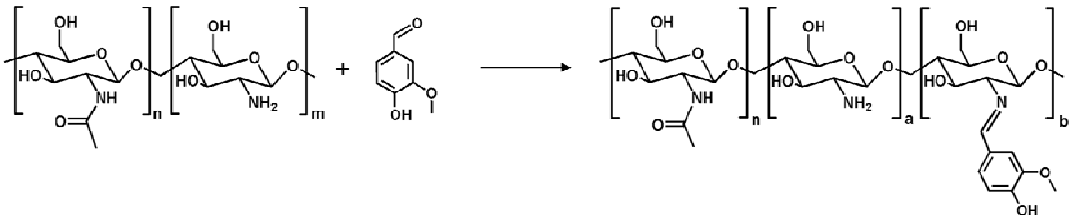

Scheme 3.2 Preparation of *N*-vanillidenechitosan

In the imine-chitosan preparation (Scheme 3.2), chitosan reacted with vanillin to produce Schiff base. The obtained product was analyzed using ATR-FTIR. The new absorption peaks at 1635 cm^{-1} corresponded to C=N stretching vibration and 1592 cm^{-1} and 1512 cm^{-1} corresponded to C=C stretching vibration of aromatic (Figure 3.9) were clearly observed.

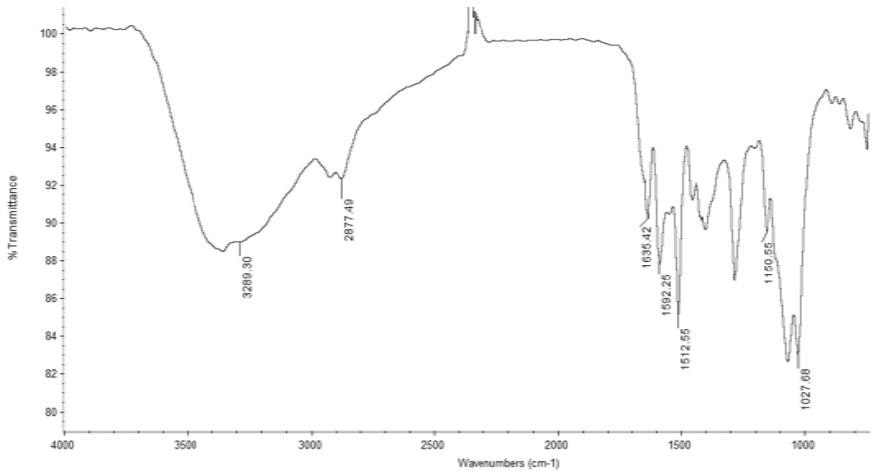

Figure 3.9 ATR-FTIR spectrum of *N*-vanillidenechitosan

3.4 Preparation of imine-N-SCS nanoparticles

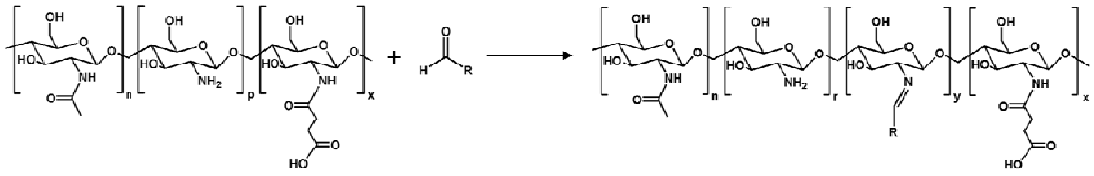

Scheme 3.3 Preparation of imine-N-SCS

Optimization condition of reaction time during imine formation

Formation of imine bond (C=N) between N-SCS nanoparticle and vanillin under heterogeneous phase reaction was determined by FT-IR spectroscopy. The new absorption band at 1635 cm^{-1} of C=N stretching confirmed the imine formation. FT-IR spectrum of reaction mixture monitored at the reaction time of 0 h did not show the C=N peak, but as expected, after 4, 8 and 25 h, the IR spectra showed new absorption peaks at 1635 cm^{-1} and 1665 cm^{-1} corresponding to C=N stretching of imine and C=O stretching of aryl aldehyde, respectively. In addition, the IR spectrum of the 25 h

reaction time showed significantly higher intensity of the peak at 1665 cm^{-1} comparing to the peak at 1635 cm^{-1}, suggesting that the imine bond formation already completed at 4 h and if the reaction was left to proceed further, hydrolysis of the imine bonds accompanied with the generation of free aldehyde would take place. FT-IR spectra of the reaction mixtures at various reaction times are shown in Figure 3.10.

Finding the optimum ratio between N-SCS nanoparticles and aldehyde

Five weight ratios of N-SCS to vanillin (5:1, 4:1, 3:1, 2:1 and 1:1) were experimented using the above optimized reaction time of 4 h. The ATR-FTIR spectra of the products indicated that additional peaks at 1635 cm^{-1} from imine and 1665 cm^{-1} from aryl aldehyde could be observed for the reaction conducted at N-SCS: vanillin weight ratio of 1:1 and 2:1 (Figure 3.11). On the other hand IR spectra of products from reactions at 3:1, 4:1 and 5:1 ratios showed only absorption band of the imine (Figure 3.11). This evidence demonstrates that the amount of aldehyde used should be at N-SCS: vanillin weight ratio of 3:1.

Various aldehydes for imine-N-SCS nanoparticles formation

The optimum condition for heterogeneous aldehydic grafting was as follows: reaction time of 4h with sonication and a weight ratio between N-SCS and vanillin of 3:1. In this thesis, two aromatic aldehydes (vanillin and cinnamaldehyde) and two aliphatic aldehydes (citronellal and citral) were used as perfumery material.

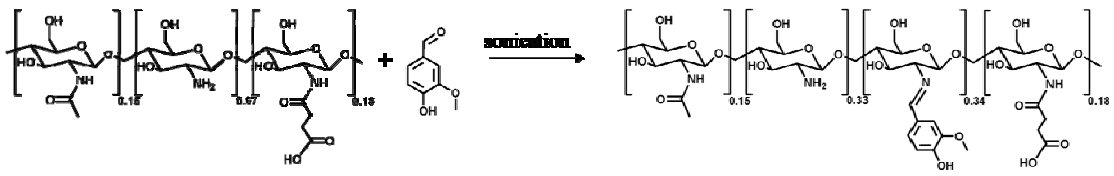

Scheme 3.4 Preparation of *N,N′*-vanillidene-succinylchitosan

The IR spectrum of *N,N′*-vanillidene-succinylchitosan showed absorption peaks at 1635 cm^{-1} and 1592 cm^{-1}, and 1512 cm^{-1} assignable to C=N stretching vibration and C=C stretching vibration of aromatic, respectively (Figure 3.12). A degree of vanillin substitution (DS) was quantitatively estimated by hydrolyzing the imine from the product, extracting the hydrolysed aldehyde, and quantitating the

amount of extracted aldehyde using UV/Vis spectroscopic analysis with the aid of calibration curve (see appendix for full details of DS determination procedure). The DS was 0.34.

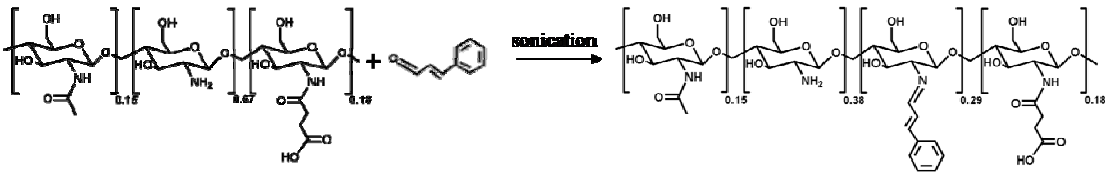

Scheme 3.5 Preparation of *N,N′*-cinnamylidene-succinylchitosan

The IR spectrum of *N,N′*-cinnamylidene-succinylchitosan showed absorption peaks at 1632 cm^{-1} and 1592 cm^{-1} assignable to C=N stretching vibration, and C=C stretching vibration of aromatic, respectively (Figure 3.13). A degree of cinnamaldehyde substitution (DS) was 0.29 (determined by the same procedure to that of *N,N′*-vanillidene-succinylchitosan).

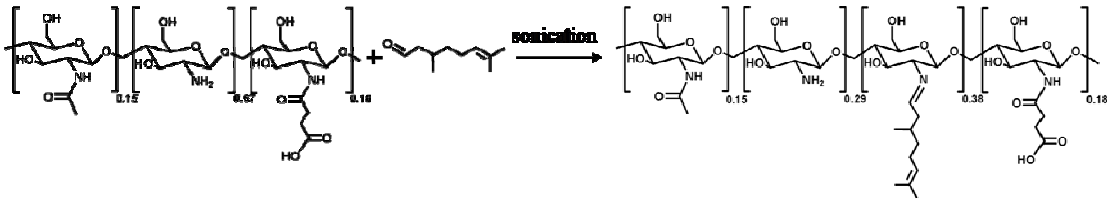

Scheme 3.6 Preparation of *N,N′*-citronellalidene-succinylchitosan

The IR spectrum of *N,N′*-citronellalidene-succinylchitosan showed absorption peaks at 1638 cm^{-1} and 1612 cm^{-1} assignable to C=N stretching vibration, and C=C stretching vibration, respectively (Figure 3.14). A degree of citronellal substitution (DS) was estimated as described above to be 0.38.

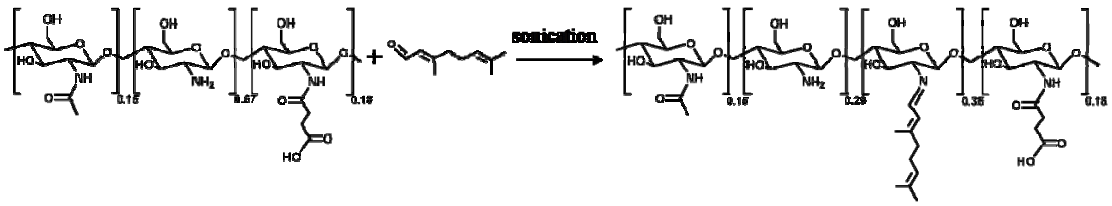

Scheme 3.7 Preparation of *N,N′*-citralidene-succinylchitosan

The IR spectrum of *N,N´*-citralidene-succinylchitosan showed absorption peaks at 1638 cm^{-1} and 1612 cm^{-1} assignable to C=N stretching vibration and C=C stretching vibration, respectively (Figure 3.15). A degree of citral substitution (DS) was 0.34.

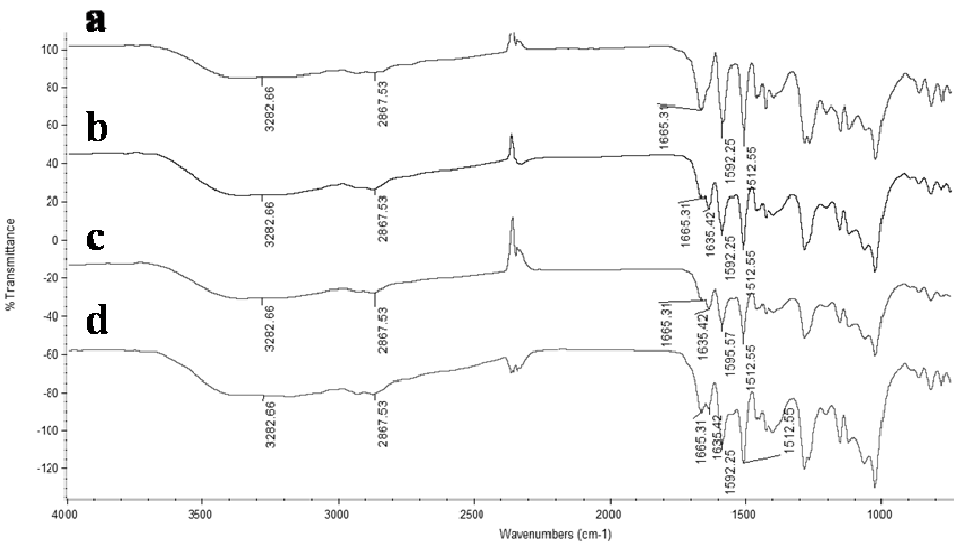

Figure 3.10 ATR-FTIR spectra of *N,N´*-vanillidene-succinylchitosan studies on imine formation at various reaction times of (a) 0, (b) 4, (c) 8 and (d) 25 h

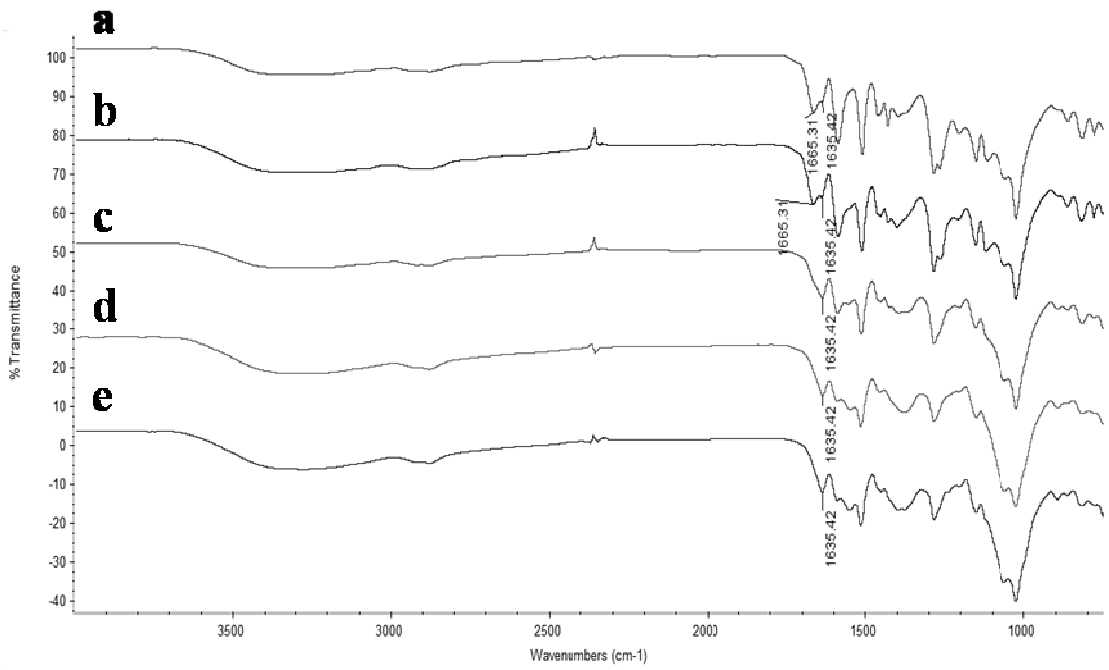

Figure 3.11 ATR-FTIR spectra of *N,N′*-vanillidene-succinylchitosan studies on imine formation at N-SCS: vanillin weight ratio of (a) 1:1, (b) 2:1, (c) 3:1, (d) 4:1 and (e) 5:1

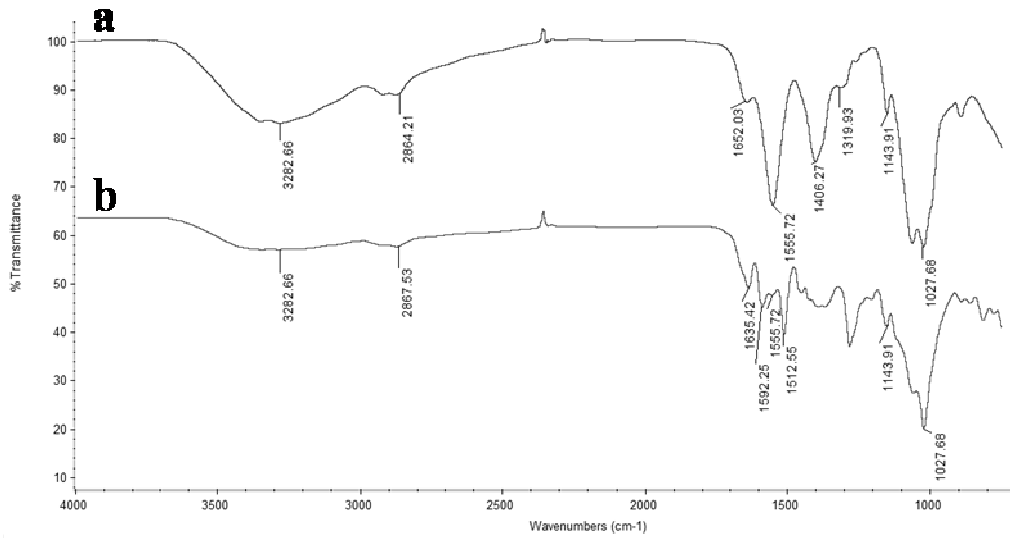

Figure 3.12 ATR-FTIR spectra of (a) N-SCS and (b) *N,N′*-vanillidene-succinylchitosan prepared at N-SCS: vanillin weight ratio of 3:1, reaction time for 4h

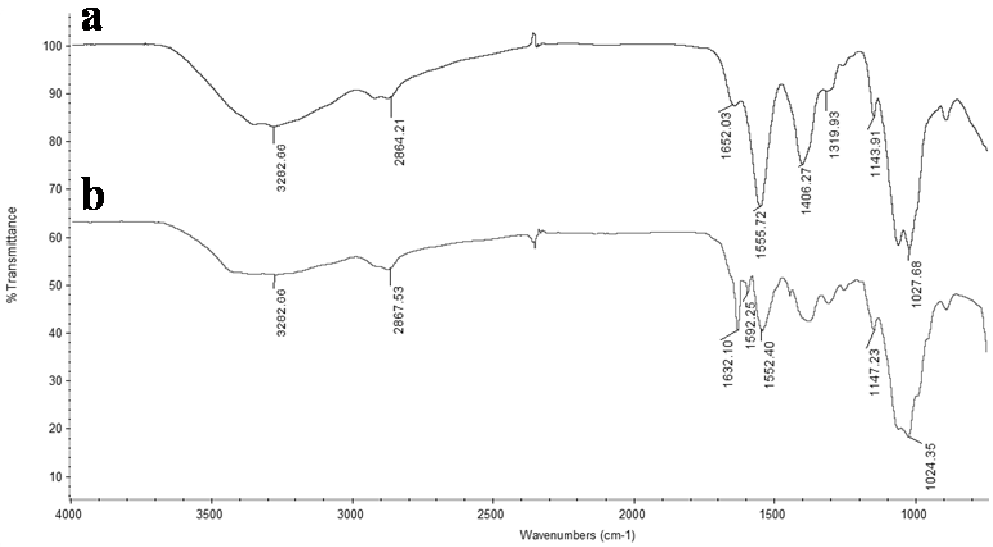

Figure 3.13 ATR-FTIR spectra of (a) N-SCS and (b) *N,N'*-cinnamylidene-succinylchitosan prepared at N-SCS: cinnamaldehyde weight ratio of 3:1, reaction time for 4h

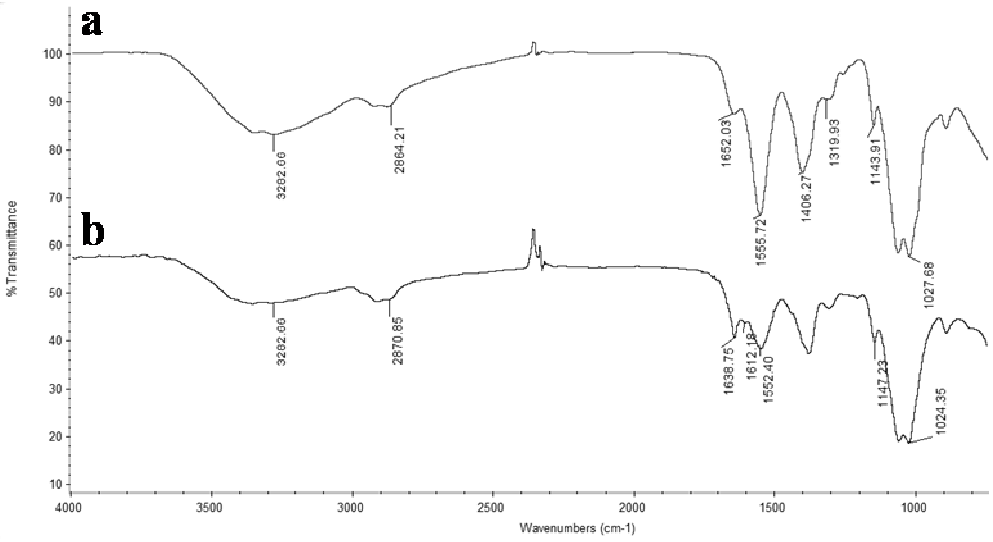

Figure 3.14 ATR-FTIR spectra of (a) N-SCS and (b) *N,N'*-citronellalidene-succinylchitosan prepared at N-SCS: citronellal weight ratio of 3:1, reaction time for 4h

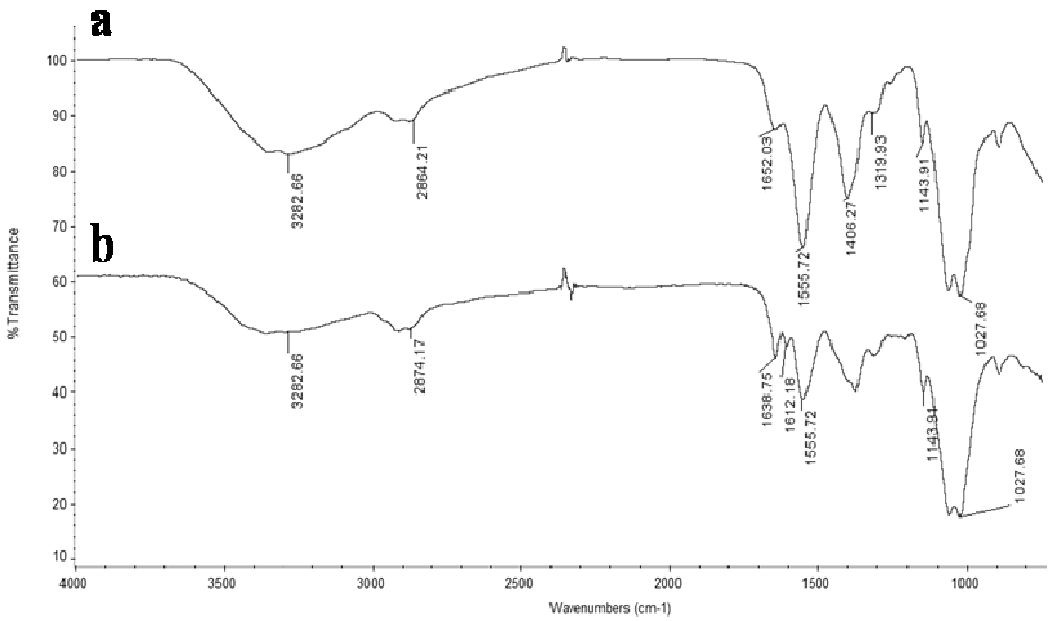

Figure 3.15 ATR-FTIR spectra of (a) N-SCS and (b) *N,N´*-citralidene-succinylchitosan prepared at N-SCS: citral weight ratio of 3:1, reaction time for 4h

Morphology, Hydrodynamic diameter and Zeta potential of the nanoparticles

The colloidal suspension of the obtained Schiff base was subject to SEM, AFM and DLS analyses. SEM photographs of *N,N´*-vanillidene-succinylchitosan (Figure 3.16) indicated size increasing after aldehyde grafting onto N-SCS nanoparticles. It should be noted here that the imine-N-SCS particles could not withstand the electron impact during SEM and TEM analyses, they burst and melt during such process, therefore their SEM images (Figure 3.16) were not clear. The AFM images, however, showed better images and it can be observed that both AFM and SEM images gave similarly spherical shape of all Schiff base N-SCS particles (Figures 3.17-3.20).

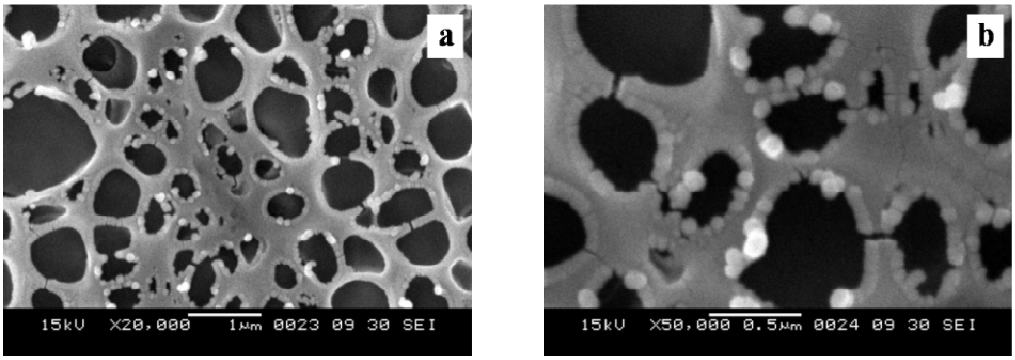

Figure 3.16 SEM photographs of *N,N´*-vanillidene-succinylchitosan nanospheres at polymer concentration of 3000 ppm (a) at 20,000xmagnification and (b) at 50,000xmagnification

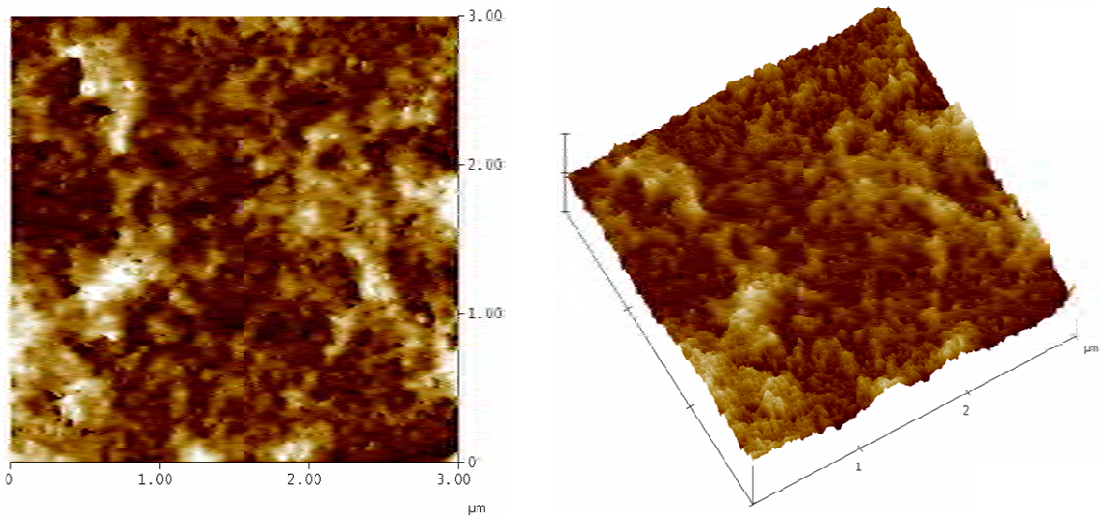

Figure 3.17 AFM images of *N,N´*-vanillidene-succinylchitosan

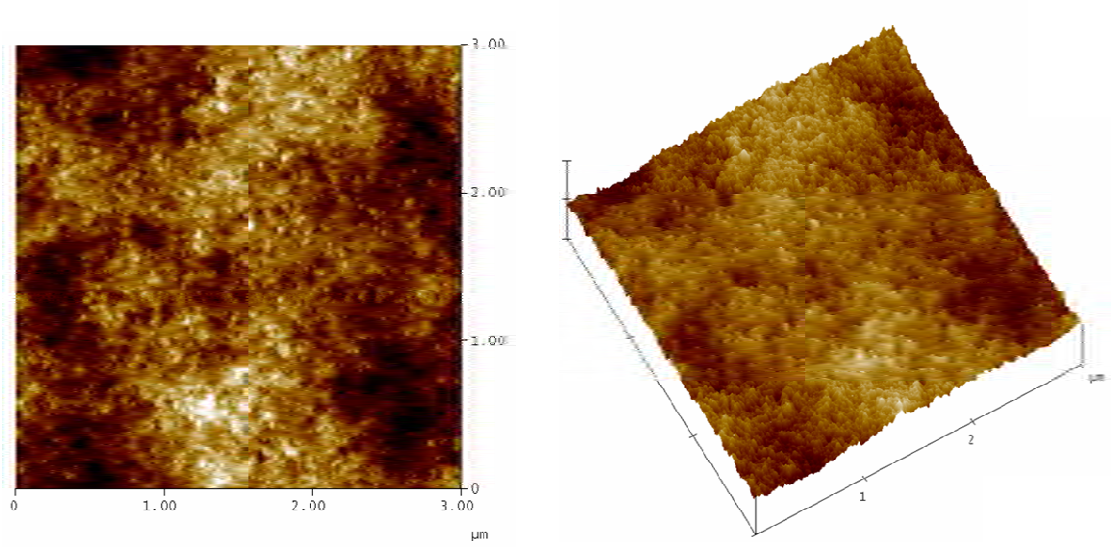

Figure 3.18 AFM images of *N*,*N*´-cinnamylidene-succinylchitosan

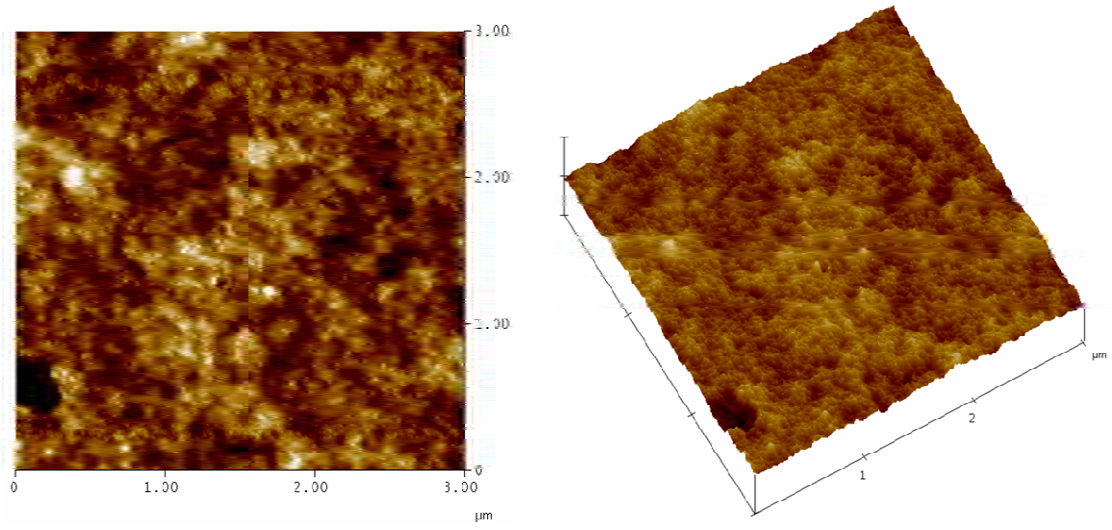

Figure 3.19 AFM images of *N*,*N*´-citronellalidene-succinylchitosan

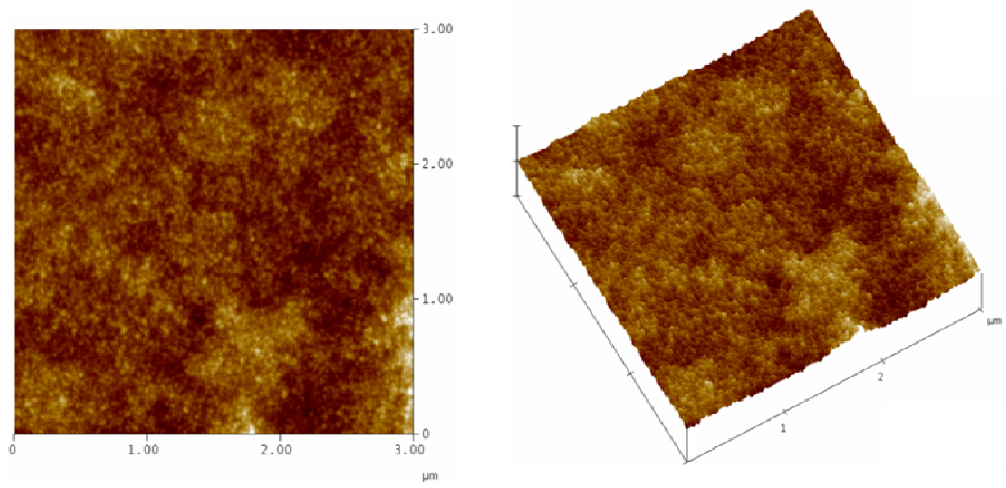

Figure 3.20 AFM images of *N*,*N*′-citralidene-succinylchitosan

Hydrodynamic diameters and polydispersity index (PDI) of the fragrant particles obtained by DLS are shown in Table 3.1. It was clear that the diameter increased from 50 nm for N-SCS particles to 80-165 nm for the Schiff base N-SCS particles and the increase could be attributed to the presence of the imine moieties. The bigger in particles size was observed in *N*,*N*′-vanillidene-succinylchitosan nanospheres and in *N*,*N*′-cinnamylidene-succinylchitosan nanospheres (as the aromatic aldehyde) when they were compared with aliphatic aldehyde nanospheres (*N*,*N*′-citronellalidene-succinylchitosan and *N*,*N*′-citralidene-succinylchitosan). It was speculated that this was a result of a difficulty in the packing of aromatic segments.

Table 3.1 Schiff base products from four perfumery aldehydes

Spheres	Hydrodynamic diameter		Zeta potential
	(nm.)	PDI	(mV)
N-succinylchitosan	46.3±0.24	0.185	+22.3 ± 2.6
N,*N*′-vanillidene-succinylchitosan	163.4 ± 2.1	0.1776	+48.8 ± 1.7
N,*N*′-cinnamylidene-succinylchitosan	130.9 ± 4.9	0.3334	+57.3 ± 4.6

Spheres	Hydrodynamic diameter		Zeta potential
	(nm.)	PDI	(mV)
N,N′-citronellalidene-succinylchitosan	109.6 ± 1.6	0.1986	+38.3 ± 2.4
N,N′-citralidene-succinylchitosan	80.9 ± 1.7	0.1668	+42.4 ± 0.6

All imine- N-SCS nanospheres show larger positive zeta potential comparing to the N-SCS nanoparticles (Table 3.1).

In theory a high negative or positive zeta potential of the nanoparticles will make them repel each other and thus minimize their aggregation. Acceptable zeta potentials of stable particles are more positive than +30 mV or more negative than -30 mV [38]. It should be noted here that the obtained zeta potentials of the obtained suspensions were above +30 mV, indicating stable suspensions obtained though aldehyde grafting on the N-SCS particles.

3.5 Micelle forming behavior

Aggregation behavior of the micelles was monitored by fluorescence spectroscopy with pyrene as a fluorescence probe. We compared two aqueous systems, N-SCS and *N,N′*-citronellalidene-succinylchitosan. The samples (the test polymer of various concentrations ranging from 0.05 to 0.60 mg/ml in the presence of pyrene) were excited at 334 nm and the emission of pyrene was recorded from 350 to 450 nm. The intensity ratio between the first peak at 372 nm (I_{372}) and the third peak at (I_{384}) of pyrene emission spectrum was used for monitoring the behavior of polymer aggregation around the pyrene molecules. The I_{372}/I_{384} value plot versus polymer concentrations was further calculated for prediction of the polymer critical aggregation concentration (cac). The method is based on the fact that fluorescent of pyrene is usually affected by the environment around pyrene molecules. The I_{372}/I_{384}

value is high when pyrene is in the hydrophilic environment. In contrast, with the aggregation of the polymer, the pyrene will be moved into the hydrophobic core of the aggregates and the value of I_{372}/I_{384} will decrease (the environment of the pyrene molecules changed from hydrophilic to hydrophobic) [39]. Figure 3.21 suggested that the cac value of *N,N'*-citronellalidene-succinylchitosan is 0.15–0.4 mg/ml. When the concentration of *N,N'*-citronellalidene-succinylchitosan is above 0.15 mg/ml, the I_{372}/I_{384} value showed more decrease comparing to that of N-SCS (see slope of the graph), agreeing with the scenario that the interior of the N-SCS is less hydrophobic than the interior of the imine-N-SCS.

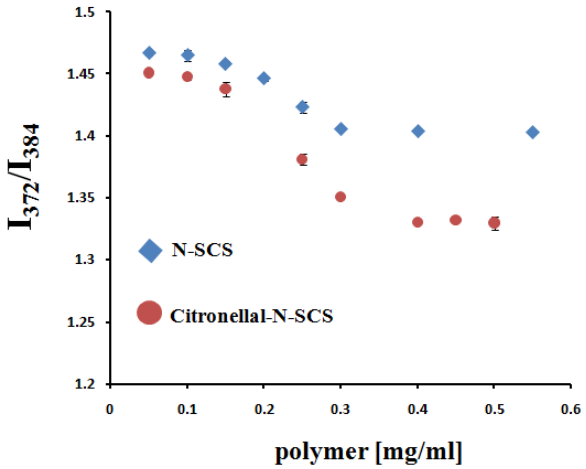

Figure 3.21 Change of intensity ratio (I_{372}/I_{384}) versus concentration of polymers (a) N-SCS and (b) *N,N'*-citronellalidene-succinylchitosan

3.6 Chemical composition at the surface

X-ray photoelectron spectroscopy (XPS) has been used for determining the chemical composition of the solid surface. It is an extremely surface sensitive technique for detecting surface modification of materials and studying the adsorption and retention of chemical agents. Information from XPS technique usually is at the surface with less than 8 nm depth.

Since the aim of this work is to create a novel controlled release system with both chemical barrier and physical barrier, it is essential to confirm the two features. The imine bond which is a chemical barrier could be clearly confirmed by IR

technique. Here we used the XPS technique to confirm the second feature which is the physical barrier. The grafted imine moieties should not be present at the surface if the physical barrier is to be claimed. In this study four samples were compared, original chitosan, self-assembled *N*-succinylchitosan nanospheres, non self-assembled *N*-vanillidenechitosan and self-assembled *N,N´*-vanillidene-succinylchitosan spheres.

The deconvoluted peaks from high resolution XPS spectra gave the surface chemical composition of prepared product as follows:

Chitosan

The C 1s core-level spectrum of chitosan could be fit into three peaks [40]: a peak at the binding energy (BE) of 285.1 eV which was assignable to C-H, the peak at the BE of 286.5 eV which was assignable to C-OH, and the peak at the BE of 287.9 eV which was assignable to both O-C-O and HN-C=O. The N 1s core-level showed two species of nitrogen: primary amine ($-NH_2$) at the BE of 399.4 eV and amide (-HN-C=O) at the BE of 400.2 eV (Figure 3.22a).

Self-assembled N-SCS spheres

The XPS spectrum of self-assembled N-SCS spheres displays new peaks at the BE of 288.5 eV (O-C=O) in the C1s spectrum and at the BE of 401.8 eV ($-NH_3^+$) in the N1s spectrum (Figure 3.22b).

Non-self-assembled N-vanillidenechitosan

For non-self-assembled Schiff base product, the XPS spectra demonstrated an additional peak of imine bond (C=N) at the BE of 285.4 and 399.1 eV, respectively (Figure 3.22c).

Self-assembled N,N´-vanillidene-succinylchitosan

In the high resolution spectra of self-assembled Schiff base spheres, the C 1s spectrum showed only four peaks assignable to C-H, C-OH, O-C-O/HN-C=O and O-C=O. Moreover, an increase in amide peak intensity also corresponded well with the grafted succinyl moiety. Very importantly, its N 1s spectrum showed only three peaks for primary amine ($-NH_2$), amide (-HN-C=O) and protonated amine ($-NH_3^+$) (Figure

3.22d), with no observable imine peak. Since the imine functionality was confirmed in the IR spectrum, this clearly indicated that the imine functionality or the grafted Schiff base were not located at the spherical surfaces (8 nm depths from the surface). Therefore, the imine functionality must be embedded at the spherical cores with the depth from the surface of more than 8 nm from the surface. Thus upon grafting, reorganization of the spheres was likely taking place in such a way that the grafted aldehyde moieties were moved into the particles' core. In addition, the great decrease in the intensity of the amine peak in the XPS spectrum of chitosan Schiff base nanospheres comparing to that of the chitosan sample corresponded well to the fact that most amine groups should have been changed into the imine functionality through the reaction with vanillin.

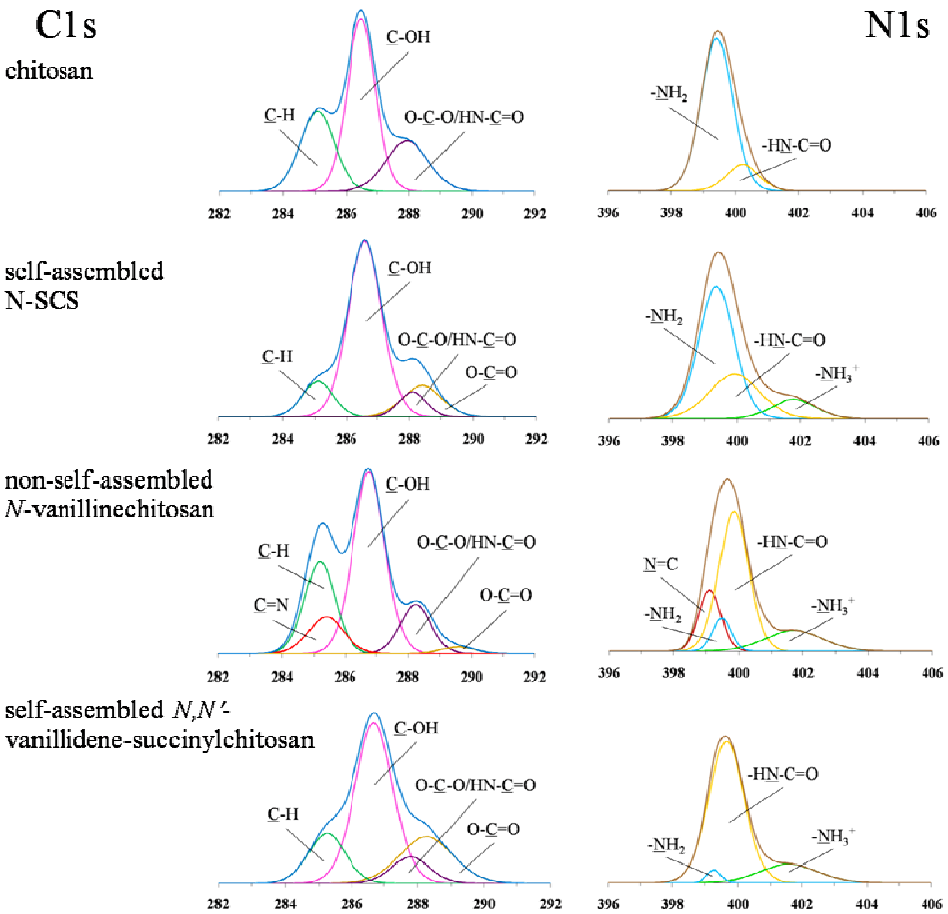

Figure 3.22 XPS high resolusion spectra of (a) chitosan, (b) self-assembled N-SCS spheres, (c) non-self-assembled *N*-vanillidenechitosan and (d) self-assembled *N,N'*-vanillidene-succinylchitosan spheres

In conclusion, all the grafted aldehydes were hydrophobic thus in the water medium they would oriented themselves away from polar environment and moved to the inside the spheres. Thus here the specific location of the grafted chemical functionality was reported for the first time for soft polymeric nanoparticles. The result confirms the frequently used theory which state that in a polar environment, amphiphilic polymer chains will self-assemble in the way that the hydrophobic moieties will be at the particles'cores while the hydrophilic moieties will be at the surface of the particles. This theory extended to the reorganization of the preformed spheres in which surface modification was carried out. It should be noted here that in fact the N-SCS particles were quite physically stable as they could hold the spherical shape upon drying, SEM, and TEM processing. Thus though the particles were physically stable, the reorganization could still take place.

3.7 The release of aldehyde from Schiff base nanoparticles

UV/Vis spectroscopic analysis

A double barrier controlled release system in this work should be able to protect the aldehyde from the external trigger and should show slow rate of aldehyde release. The release mechanism involves diffusion of water into the spheres, the imine hydrolysis, and the diffusion of the hydrolysed aldehydes out of the spheres. To investigate effect of aldehyde structure on the release rate, both aromatic (vanillin and cinnamaldehyde) and aliphatic aldehydes (citronellal and citral) were employed. We examined the release of aldehyde by quantitating the remaining aldehyde molecules. Hexane extraction coupled with acid hydrolysis was used to quantitate the remaining aldehyde. As shown in Figures 3.23-3.26, the remaining amount of aldehyde decreased with passing times. All release profiles indicated sustained aldehyde release for the Schiff base nanoparticles comparing to free aldehyde.

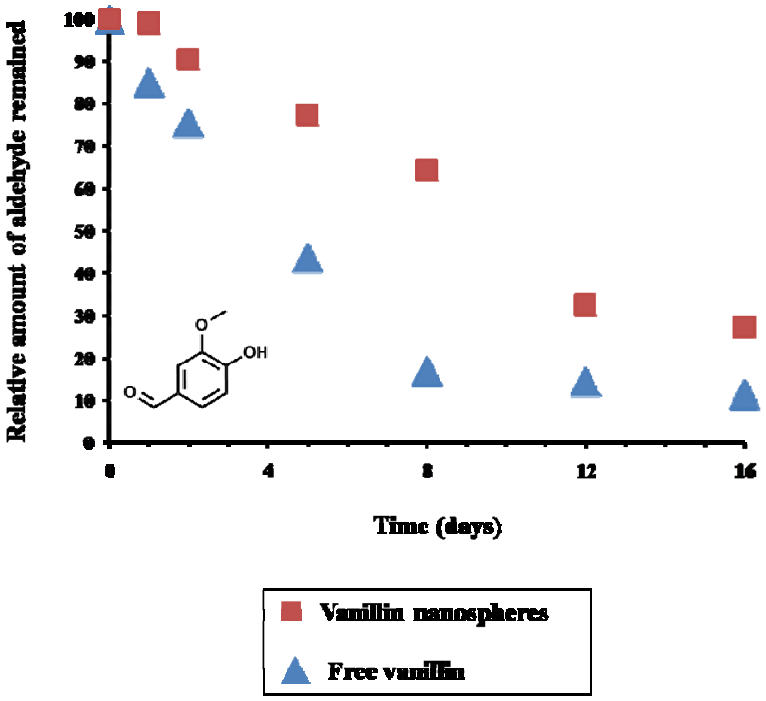

Figure 3.23 Time versus amount of vanillin remained from Schiff base nanospheres compared with free vanillin

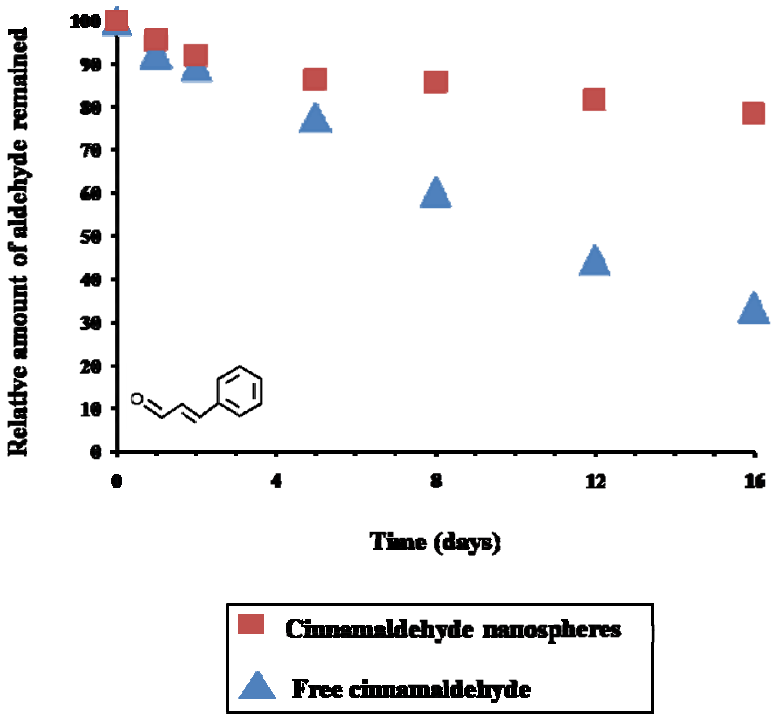

Figure 3.24 Time versus amount of cinnamaldehyde remained from Schiff base nanospheres compared with free cinnamaldehyde

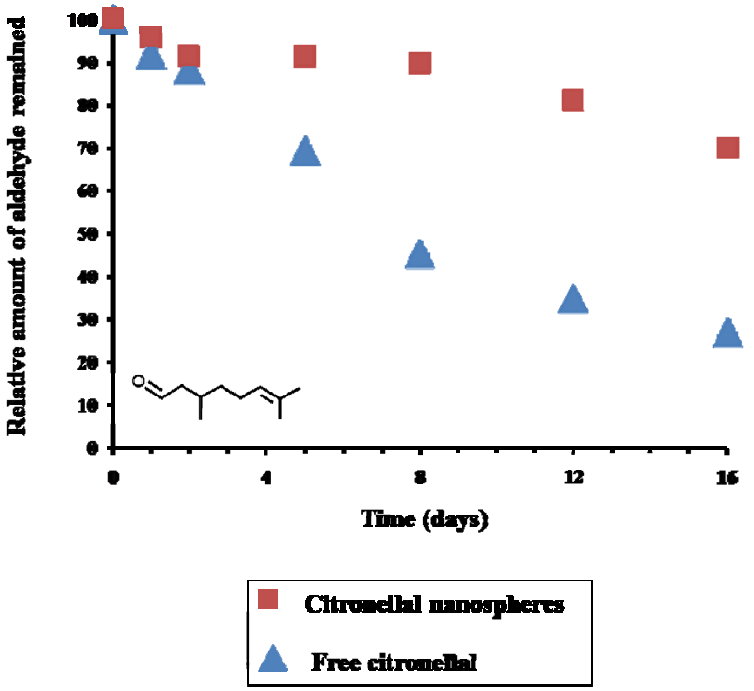

Figure 3.25 Time versus amount of citronellal remained from Schiff base nanospheres compared with free citronellal

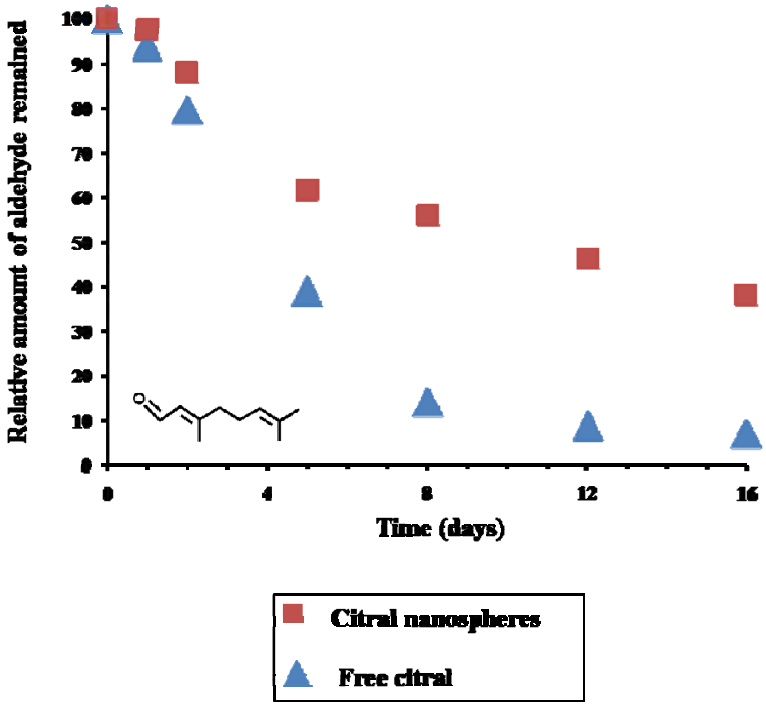

Figure 3.26 Time versus amount of citral remained from Schiff base nanospheres compared with free citral

Some applications of fragrance aldehydes would involve dry condition, the release of the fragrance aldehydes from the dry samples was evaluated after 60 days (some 40 days as dry samples) at 40 ^{O}C. Hydrolysis of the samples followed with aldehyde quantification indicated (Mean $\pm$ S.D.) 2.88 ± 0.20, 0.77 ± 0.02, 4.52 ± 0.31 and 1.31 ± 0.10 mg of vanillin, cinnamaldehyde, citronellal and citral in the corresponding imine-N-SCS samples, which was significantly higher (79.9-, 85.4-, 20.1- and 29.1-fold, respectively) than the free aldehyde levels in the control samples at 0.036 ± 0.001, 0.009 ± 0.002, 0.225 ± 0.092 and 0.045 ± 0.002 mg of vanillin, cinnamaldehyde, citronellal and citral, respectively. Comparing this result to those in aqueous state, the dry Schiff base nanospheres were un-swelled thus making the difficult and slow penetration of water molecules into the inside of the particles where the imine linkages located. It was obvious that the prolonged release of the double barrier-carriers was much more pronounced in the dry state.

CHAPTER IV

CONCLUSION

A new carrier from chitosan derivative having a double barrier (physical and chemical barriers) for controlled release of aldehyde was prepared. The physical barrier was simply made by self-assembly of *N*-succinylchitosan (N-SCS) with degree succinyl substitution of 0.18 to obtain transparent colloidal suspension, and a chemical barrier involved imine formation from the grafting reaction of representative aromatic (vanillin and cinnamaldehyde) and aliphatic (citronellal and citral) perfumery aldehydes onto amino group of N-SCS nanoparticles. All four Schiff base products, *N*,*N*′-vanillidene-succinylchitosan, *N*,*N*′-cinnamylidene-succinylchitosan, *N*,*N*′-citronellalidene-succinylchitosan and *N*,*N*′-citralidene-succinylchitosan, had a degree of imine substitution in the range of 0.29-0.38. The obtained products remain spherical shape and the particle size determined from DLS increased from 50 nm for N-SCS to 80-165 nm for Schiff base products. It is necessary for investigation the location of imine moieties in order to claim the physical barrier and to predict the difficulty of chemical barrier hydrolysis. X-ray photoelectron spectroscopic analysis (XPS) results suggested that amino groups of N-SCS were at the particle surface. After reaction between aldehyde molecules and amino groups at the surface to form imine, the grafted imine moved to the inside of the spheres. Release profiles of aldehydes from all Schiff base nanospheres in both aqueous suspension and dry state clearly indicated prolonged release of the aldehyde comparing to the system of free aldehyde. The controlled release system based on a double barrier carrier not only gave an applicable fragrance controlled release system, but also demonstrated that reorganization of the soft polymeric nanoparticles could be taking place upon surface modification. This reorganization possibility should be applicable to the design of other novel nanostructured materials.

REFERENCES

[1] Gautschi, M., Bajgrowicz, J. A., and Kraft, P., Fragrance chemistry-milestones and perspectives. *CHIMIA International Journal for Chemistry*, 55, 5(2001): 379-387.

[2] Madene, A., Jacquot, M., Scher, J., and Desobry, S., Flavour encapsulation and controlled release. *International Journal of Food Science & Technology*, 41, (2006): 1-21.

[3] Morinaga, H., Morikawa, H., Wang, Y., Sudo, A., and Endo, T., Amphiphilic copolymer having acid-Labile acetal in the side chain as a hydrophobe: controlled release of aldehyde by thermoresponsive aggregation-dissociation of polymer micelles. *Macromolecules*, 42, 6(2009): 2229-2235.

[4] Rudzinski, W. E., Chipuk, T., Dave, A. M., Kumbar, S. G., and Aminabhavi, T. M., pH-sensitive acrylic-based copolymeric hydrogels for the controlled release of a pesticide and a micronutrient. *Journal of Applied Polymer Science*, 87, 3(2003): 394-403.

[5] Sansukcharearnpon, A., Wanichwecharungruang, S., Leepipatpaiboon, N., Kerdcharoen, T., and Arayachukeat, S., High loading fragrance encapsulation based on a polymer-blend: Preparation and release behavior. *International Journal of Pharmaceutics*, 391, 1-2(2010): 267-273.

[6] Robles, J.L., and Bochet, C.G., Photochemical release of aldehydes from α-acetoxy nitroveratryl ethers. *Organic Letters*, 7, 16(2005): 3545-3547.

[7] Levrand, B., Ruff, Y., Lehn, J.M., and Herrmann, A., Controlled release of volatile aldehydes and ketones by reversible hydrazone formation ‘‘classical’’ profragrances are getting dynamic. *Chemical Communications*, 28(2006): 2965-2967.

[8] Eilerman, R.G., Christenson, P.A., Yurecko, J. M. Jr., Mild, F., and Kucharski, P.E., Novel cyclic acetals. *European Patent 0413162*, (1991).

[9] Powell, K., Benkhoff, J., Fischer, W., and Fritzsche, K., Secret sensations: Novel functionalities triggered by light - Part II: Photolatent fragrances. *European Coatings Journal*, 9, (2006): 40-49.

[10] Rochat, S., Minardi, C., de Saint Laumer, J.Y., and Herrmann, A., Controlled release of perfumery aldehydes and ketones by Norrish Type-II photofragmentation of alpha-keto esters in undegassed solution. *Helvetica Chimica Acta*, 83, 7(2000): 1645-1671.

[11] Yang, Y., Wahler, D., and Reymond, J.L., *β*-Amino alcohol properfumes. *Helvetica Chimica Acta*, 86, 8(2003): 2928-2936.

[12] Forestier, J. P., Les enzymes de l'espace extra-cellulaire du stratum corneum. *International Journal of Cosmetic Science*, 14, 2(1992): 47-63.

[13] Jaeger, K.E., et al., Bacterial lipases. *FEMS Microbiology Reviews*, 15, 1(1994): 29-63.

[14] Aulenta, F., et al., Fragrance release from the surface of branched Poly (Amide) S. *Molecules*, 10, 1(2005): 81-97.

[15] Anderson, D., and Frater, G., Beta ketoesters. *European Patent 0911315*, (1999).

[16] Herrmann, A., Controlled release of volatiles under mild reaction conditions: From nature to everyday products. *Angewandte Chemie International Edition*, 46, 31(2007): 5836-5863.

[17] Waliszewski, K.N., Pardio, V.T., and Ovando, S.L., A simple and rapid HPLC technique for vanillin determination in alcohol extract. *Food Chemistry*, 101, 3(2007): 1059-1062.

[18] Ponce Cevallos, P.A., Buera, M.P., and Elizalde, B.E., Encapsulation of cinnamon and thyme essential oils components (cinnamaldehyde and thymol) in β-cyclodextrin: Effect of interactions with water on complex stability. *Journal of Food Engineering*, 99, 1(2010): 70-75.

[19] Sakulku, U., et al., Characterization and mosquito repellent activity of citronella oil nanoemulsion. *International Journal of Pharmaceutics*, 372, 1-2(2009): 105-111.

[20] Choi, S.J., Decker, E.A., Henson, L., Popplewell, L.M., and McClements, D.J., Inhibition of citral degradation in model beverage emulsions using micelles and reverse micelles. *Food Chemistry*, 122, 1(2010): 111-116.

[21] Kamogawa, H., Mukai, H., Nakajima, Y., and Nanasawa, M., Chemical release control-Schiff bases of perfume aldehydes and aminostyrenes. *Journal of Polymer Science: Polymer Chemistry Edition*, 20, 11(1982): 3121-3129.

[22] Wade, L.G., Organic Chemistry. sixth edition, Upper Saddle River, New Jersey: Pearson Prentice Hall, 2006.

[23] Hsieh, W.C., Chang, C.P., and Gao, Y.L., Controlled release properties of chitosan encapsulated volatile citronella oil microcapsules by thermal treatments. *Colloids and Surfaces B: Biointerfaces*, 53, 2(2006): 209-214.

[24] Numanoğlu, U., et al., Use of cyclodextrins as a cosmetic delivery system for fragrance materials: Linalool and benzyl acetate. *AAPS PharmSciTech*, 8, 4(2007).

[25] Wang, P., Zhu, Y., Yang, X., and Chen, A., Prolonged-release performance of perfume encapsulated by tailoring mesoporous silica spheres. *Flavour and Fragrance Journal*, 23, (2008): 29-34.

[26] Theisinger, S., Schoeller, K. Osborn, B., Sarkar, M., and Landfester, K., Encapsulation of a fragrance via miniemulsion polymerization for temperature-controlled release. *Macromolecular Chemistry and Physics*, 210, (2009): 411-420.

[27] Muzzarelli, R., and Muzzarelli, C., Chitosan Chemistry: Relevance to the biomedical sciences. *Advances in Polymer Science*, 186, (2005): 151-209.

[28] Kurita, K., Chitin and chitosan: Functional biopolymers from marine crustaceans. *Marine Biotechnology*, 8, 3(2006): 203-226.

[29] Harish Prashanth, K.V., and Tharanathan, R.N., Chitin/chitosan: modifications and their unlimited application potential--an overview. *Trends in Food Science & Technology*, 18, 3(2007):117-131.

[30] Pillai, C.K.S., Paul, W., and Sharma, C.P., Chitin and chitosan polymers: Chemistry, solubility and fiber formation. *Progress in Polymer Science*, 34, 7(2009): 641-678.

[31] Hu, Y., et al., Synthesis and characterization of chitosan-poly(acrylic acid) nanoparticles. *Biomaterials*, 23, 15(2002): 3193-3201.

[32] Yoksan, R., Matsusaki, M., Akashi, M., and Chirachanchai, S., Controlled hydrophobic/hydrophilic chitosan: Colloidal phenomena and nanosphere formation. *Colloid & Polymer Science*, 282, 4(2004): 337-342.

[33] Ye, W., et al., Novel core-shell particles with poly(n-butyl acrylate) cores and chitosan shells as an antibacterial coating for textiles. *Polymer*, 46, 23(2005): 10538-10543.

[34] Aiping, Z., Tian, C., Lanhua, Y., Hao, W., and Ping, L., Synthesis and characterization of N-succinyl-chitosan and its self-assembly of nanospheres. *Carbohydrate Polymers*, 66, 2(2006): 274-279.

[35] Hoven, V.P., Tangpasuthadol, V., Angkitpaiboon, Y., Vallapa, N., and Kiatkamjornwong, S., Surface-charged chitosan: Preparation and protein adsorption. *Carbohydrate Polymers*, 68, 1(2007): 44-53.

[36] Yoksan, R., Jirawutthiwongchai, J., and Arpo, K., Encapsulation of ascorbyl palmitate in chitosan nanoparticles by oil-in-water emulsion and ionic gelation processes. *Colloids and Surfaces B: Biointerfaces*, 76, 1(2010): 292-297.

[37] Zhu, A., Chan Park, M.B., Dai, S., and Li, L., The aggregation behavior of O-carboxymethylchitosan in dilute aqueous solution. *Colloids and Surfaces B: Biointerfaces*, 43, 3-4(2005): 143-149.

[38] Muller, R.H., Jacobs, C., and Kayser, O., Nanosuspensions as particulate drug formulations in therapy: Rationale for development and what we can expect for the future. *Advanced Drug Delivery Reviews*, 47, 1(2001): 3-19.

[39] Vorobyova, O., Yekta, A., Winnik, M.A., and Lau, W., Fluorescent probe studies of the association in an aqueous solution of a hydrophobically modified poly(ethylene oxide). *Macromolecules*, 31, 25(1998): 8998-9007.

[40] Tang, F., Zhang, L., Zhu, J., Cheng, Z., and Zhu, X., Surface functionalization of chitosan nanospheres via surface-initiated AGET ATRP mediated by

iron catalyst in the presence of limited amounts of air. *Industrial & Engineering Chemistry Research*, 48, 13(2009): 6216-6223.

APPENDIX

1. Determination of degree of succinyl substitution

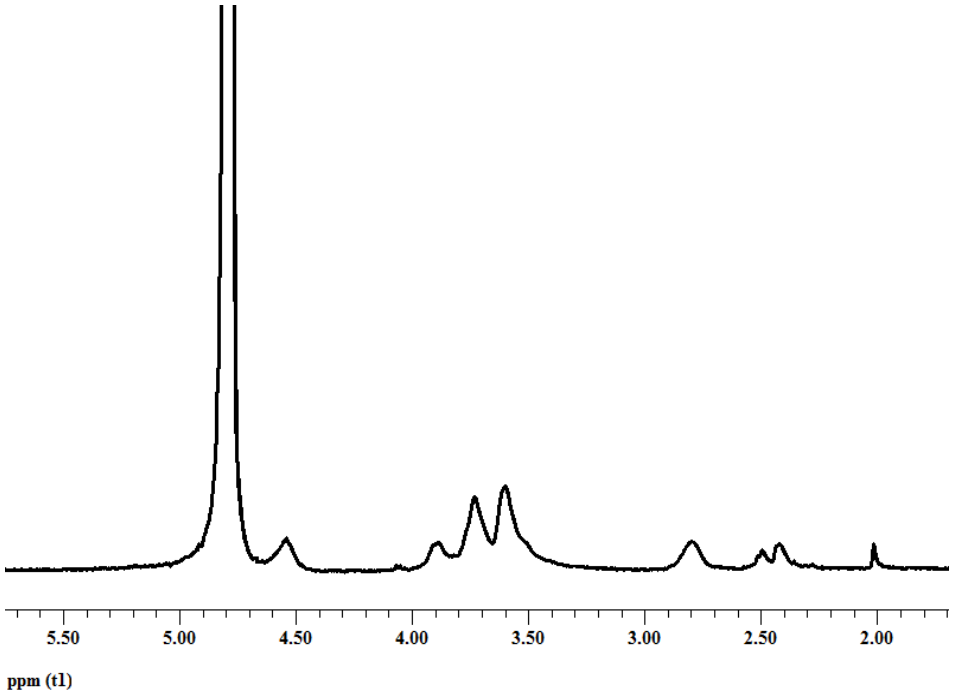

Figure A1. ^{1}H NMR spectrum of *N*-succinylchitosan2 (N-SCS2)

The degree of grafting could be determined using equation (1):

$$DG = \frac{I_{graft} \text{ x } DD}{n \text{ x } I_{cs}} \quad (1)$$

I_{graft} = the intensity of grafted moiety
DD = the amount of deacetylation degree
n = number of protons of grafted moiety
I_{cs} = the intensity of hydrogen atom of chitosan's glucosamine unit

From the ^{1}H NMR spectrum (Figure A1), using the integral ratio between 4H from ethyl group of succinyl (2.42-2.50 ppm) and 1H from C2 of glucosamine unit (at 2.8 ppm) with 85% deacetylation degree:

$$DG = \frac{0.86 \text{ x } 0.85}{4 \text{ x } 1}$$

$$DG = 0.18$$

The degree of succinyl substitution could be estimated as 0.18.

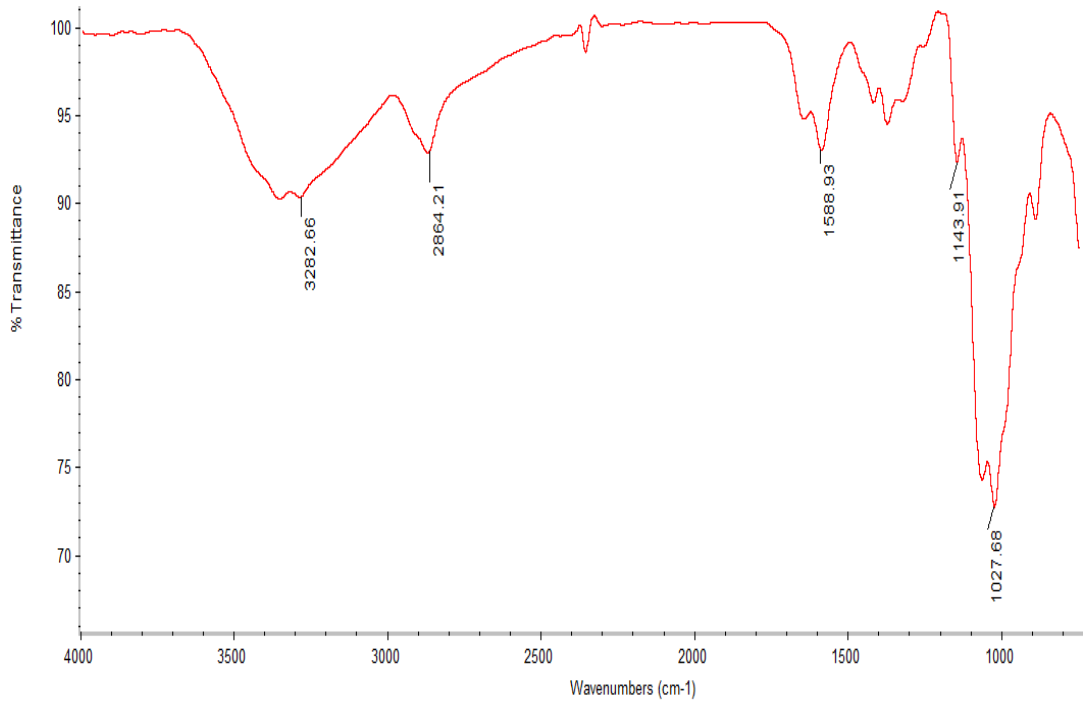

Figure A2. ATR-FTIR spectrum of chitosan

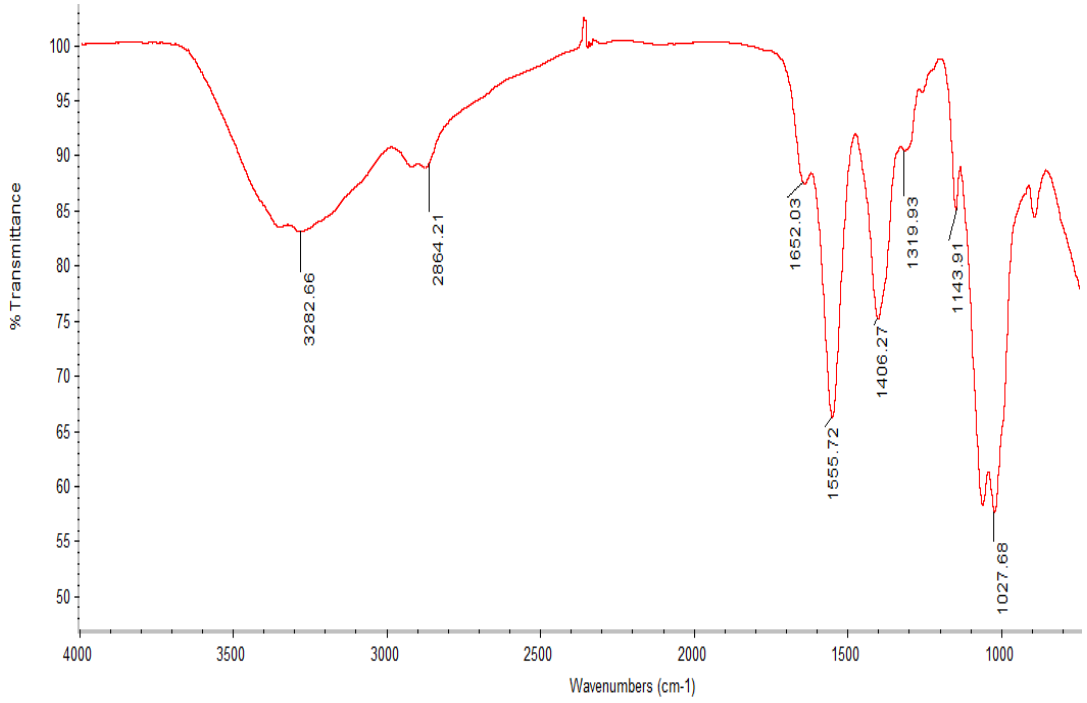

Figure A3. ATR-FTIR spectrum of *N*-succinylchitosan (N-SCS)

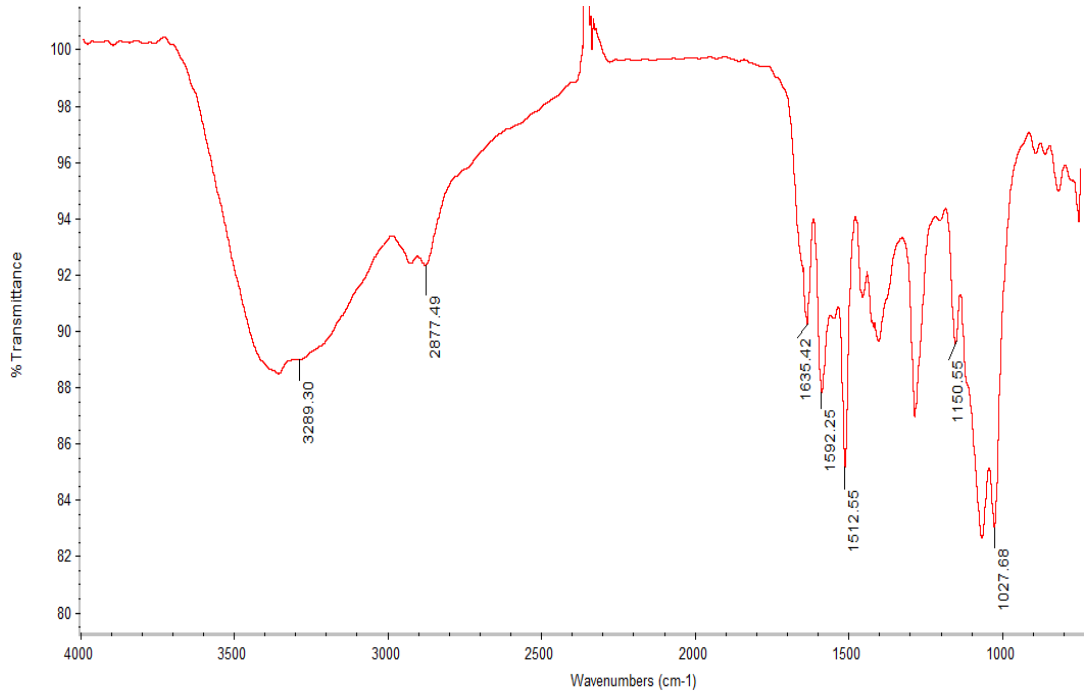

Figure A4. ATR-FTIR spectrum of *N*-vanillidenechitosan

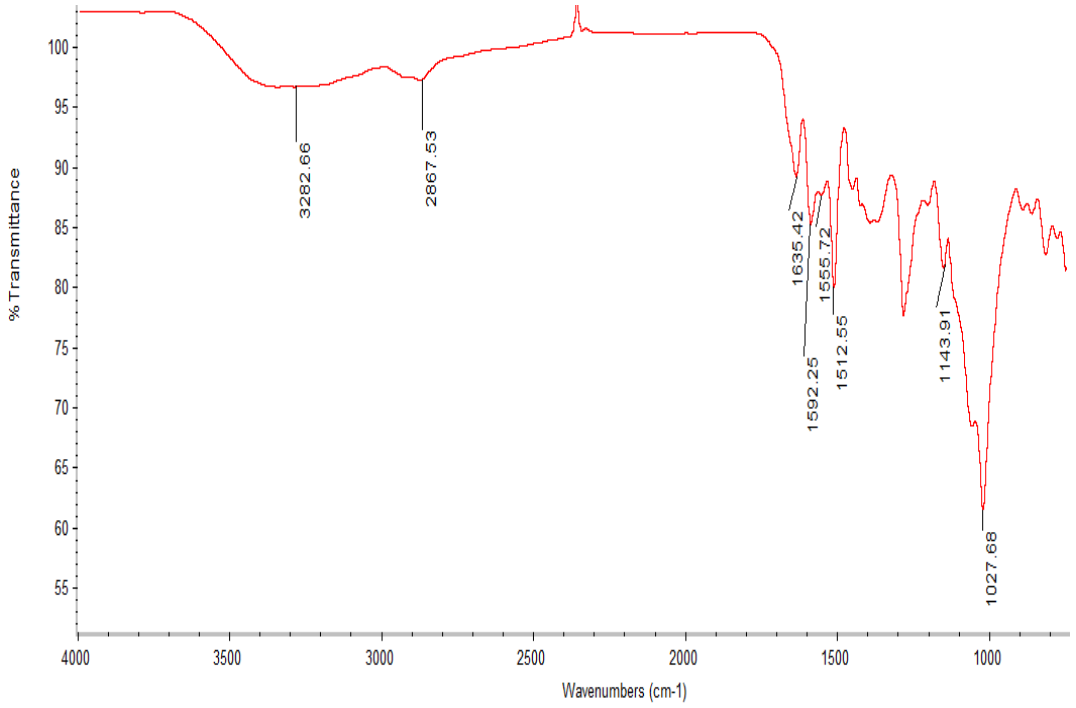

Figure A5. ATR-FTIR spectrum of *N*,*N*′-vanillidene-succinylchitosan

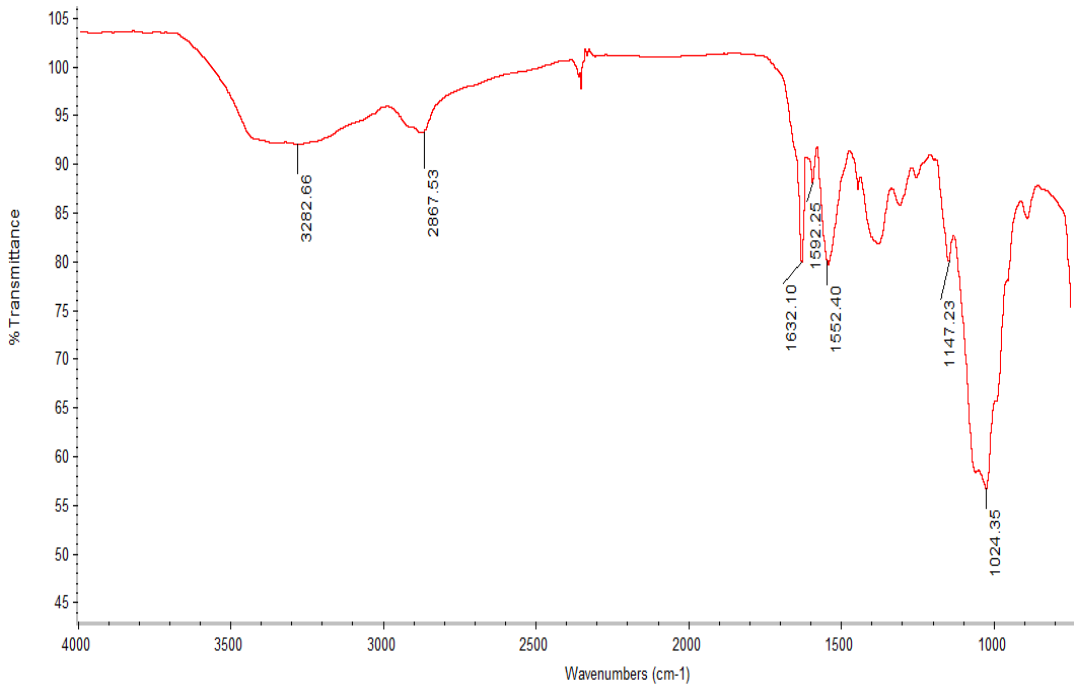

Figure A6. ATR-FTIR spectrum of *N,N′*-cinnamylidene-succinylchitosan

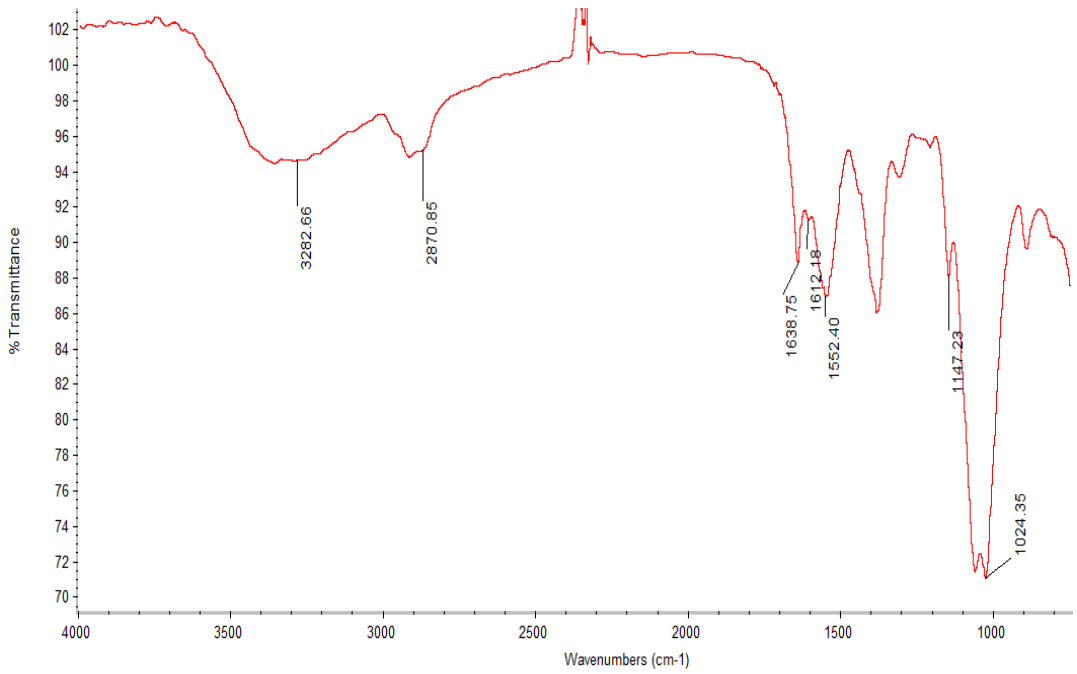

Figure A7. ATR-FTIR spectrum of *N,N′*-citronellalidene-succinylchitosan

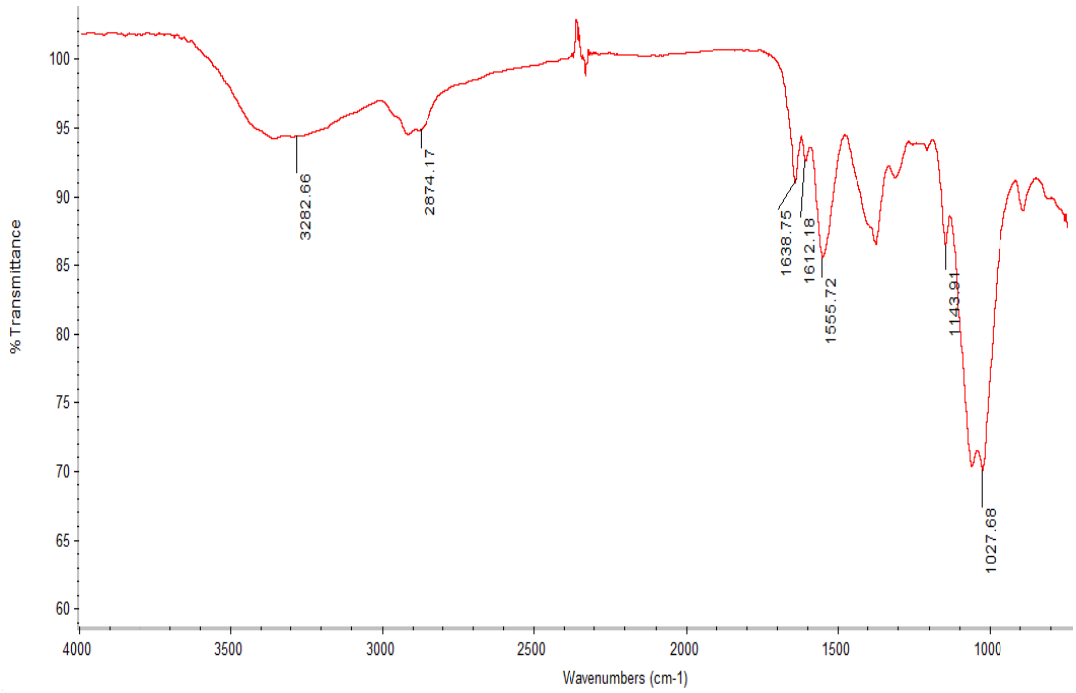

Figure A8. ATR-FTIR spectrum of *N,N'*-citralidene-succinylchitosan

2. Determination of degree of aldehyde moiety grafting (imine functionality)

2.1 Degree of vanillin grafting on the N-SCS

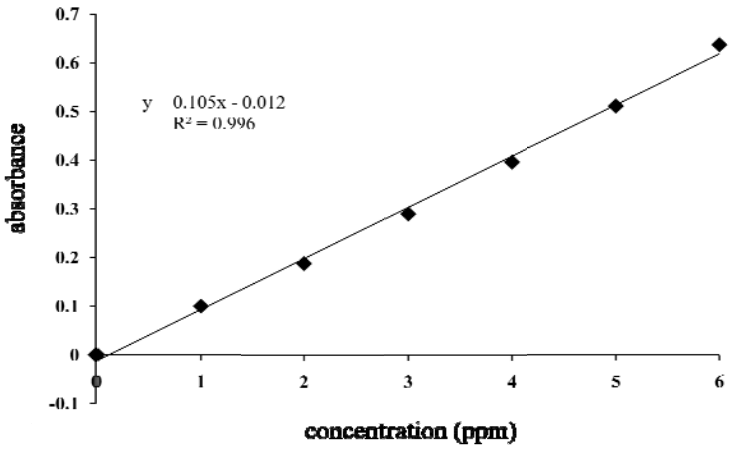

Figure A9. Calibration curve of vanillin at 269 nm

The amount of extracted vanillin from *N,N'*-vanillidene-succinylchitosan was estimated with the aid of the calibration curve:

$$Y = 0.105X - 0.012 \quad (2)$$

From equation (2) $0.491 = 0.105X - 0.012$

X = 4.79 ppm

Dilution factor = 143

X = 4.79 x 143

X = 685 ppm

Weight of grafted vanillin in 15 mL = 685 x 0.015

= 10.28 mg

Molecular weight of vanillin = 152.15 mg/mol

∴ Mole of vanillin = 10.28/152.15 = 0.068 mol

The amount of N-SCS = 37.5 mg, molecular weight = 185.30

∴ Mole of N-SCS = 37.5/185.30 = 0.202 mol

Degree of grafting (DG) = mol of grafted moiety/mol of N-SCS

DG = 0.068/0.202 = 0.34

The degree of vanillin grafting could be estimated as 0.34.

2.2 Degree of cinnamaldehyde grafting on the N-SCS

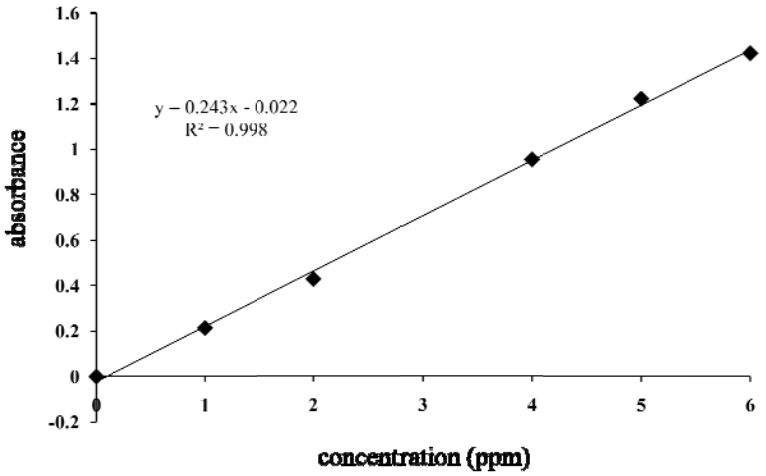

Figure A10. Calibration curve of cinnamaldehyde at 279 nm

The amount of extracted cinnamaldehyde from *N,N'*-cinnamylidene-succinylchitosan was estimated with the aid of the calibration curve:

Y = 0.243X - 0.022 (3)

From equation (3) 0.465 = 0.243X - 0.022

X = 2.004 ppm

Dilution factor = 333

X = 2.004 x 333

X = 668 ppm

Weight of grafted cinnamaldehyde in 15 mL = 668 x 0.015

= 10.02 mg

Molecular weight of cinnamaldehyde = 132.16 mg/mol

∴ Mole of cinnamaldehyde = 10.02/132.16 = 0.076 mol

The amount of N-SCS = 37.5 mg, molecular weight = 185.30

∴ Mole of N-SCS = 37.5/185.30 = 0.202 mol

Degree of grafting (DG) = mol of grafted moiety/mol of N-SCS

DG = 0.076/0.202 = 0.38

The degree of cinnamaldehyde grafting could be estimated as 0.38.

2.3 Degree of citronellal grafting on the N-SCS

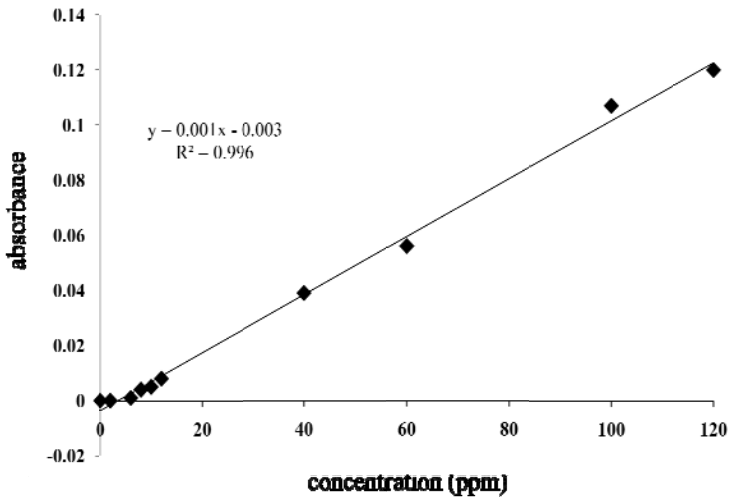

Figure A11. Calibration curve of citronellal at 231 nm

The amount of extracted citronellal from *N,N'*-citronellalidene-succinylchitosan was estimated with the aid of the calibration curve:

Y = 0.001X - 0.003 (4)

From equation (4) 0.6 = 0.001X - 0.003

X = 603 ppm

Weight of grafted citronellal in 15 mL = 603 x 0.015

= 9.045 mg

Molecular weight of citronellal = 154.25 mg/mol

∴ Mole of citronellal = 9.045/154.25 = 0.059 mol

The amount of N-SCS = 37.5 mg, molecular weight = 185.30

∴ Mole of N-SCS = 37.5/185.30 = 0.202 mol

Degree of grafting (DG) = mol of grafted moiety/mol of N-SCS

DG = 0.059/0.202 = 0.29

The degree of citronellal grafting could be estimated as 0.29.

2.4 Degree of citral grafting on the N-SCS

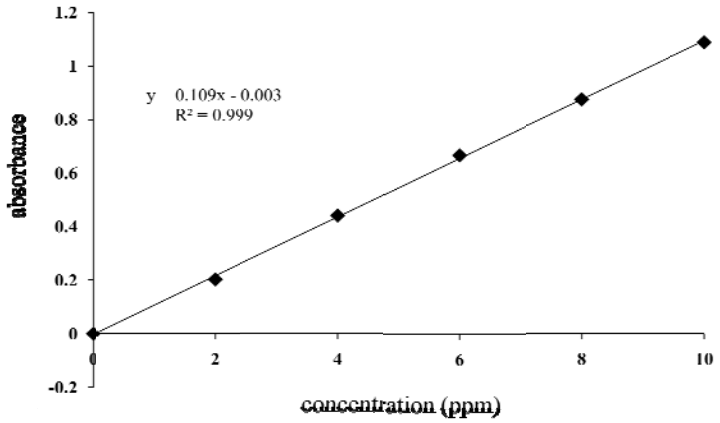

Figure A12. Calibration curve of citral at 232 nm

The amount of extracted citral from *N,N′*-citralidene-succinylchitosan was estimated with the aid of calibration curve

$$Y = 0.109X - 0.003 \quad (5)$$

From equation (5) $0.634 = 0.109X - 0.003$

$X = 5.84$ ppm

Dilution factor = 100

$X = 5.84 \times 100$

$X = 584$ ppm

Weight of grafted citral in 15 mL = 584 x 0.015

= 8.76 mg

Molecular weight of citral = 154.25 mg/mol

∴ Mole of citral = 8.76/154.25 = 0.058 mol

The amount of N-SCS = 37.5 mg, molecular weight = 185.30

∴ Mole of N-SCS = 37.5/185.30 = 0.202 mol

Degree of grafting (DG) = mol of grafted moiety/mol of N-SCS

DG = 0.058/0.202 = 0.29

The degree of citral grafting could be estimated as 0.29

3. Controlled release study

3.1 The amount of remained vanillin

- *Vanillin from hydrolysis of nanoparticles suspension at 0 day*

From equation (2) Y = 0.105X - 0.012

0.491 = 0.105X - 0.012

X = 4.79

Dilution factor = 143

X = 4.79 x 143

X = 685 ppm

Weight of vanillin in 15 mL = 685 x 0.015

= 10.28 mg

∴ Relative amount of vanillin remained at 0 day = (10.28/10.28)x100

= 100%

- *Vanillin from hydrolysis of nanoparticles suspension at 16 day*

From equation (2) Y = 0.105X - 0.012

0.125 = 0.105X - 0.012

X = 1.30

Dilution factor = 143

X = 1.30 x 143

X = 185.9 ppm

Weight of vanillin in 15 mL = 185.9 x 0.015

= 2.80 mg

∴ Relative amount of vanillin remained at 16 day = (2.80/10.28)x100

= 27.20%

- *Vanillin from hydrolysis of free aldehyde solution at 0 day*

From equation (2) Y = 0.105X - 0.012

$$0.517 = 0.105X - 0.012$$

$$X = 5.04$$

Dilution factor = 143

$$X = 5.04 \times 143$$

$$X = 721 \text{ ppm}$$

Weight of vanillin in 15 mL = 721 x 0.015

= 10.81 mg

∴ Relative amount of vanillin remained at 0 day = (10.81/10.81)x100

= 100%

- *Vanillin from hydrolysis of free aldehyde solution at 16 day*

From equation (2) $Y = 0.105X - 0.012$

$$0.047 = 0.105X - 0.012$$

$$X = 0.562$$

Dilution factor = 143

$$X = 0.562 \times 143$$

$$X = 80.37 \text{ ppm}$$

Weight of vanillin in 15 mL = 80.37 x 0.015

= 1.21 mg

∴ Relative amount of vanillin remained at 16 day = (1.21/10.81)x100

= 11.20%

3.2 The amount of remained cinnamaldehyde

- *Cinnamaldehyde from hydrolysis of nanoparticles suspension at 0 day*

From equation (3) $Y = 0.243X - 0.022$

$$0.465 = 0.243X - 0.022$$

$$X = 2.004$$

Dilution factor = 333

$$X = 2.004 \times 333$$

$$X = 668 \text{ ppm}$$

Weight of cinnamaldehyde in 15 mL = 668 x 0.015

= 10.02 mg

∴ Relative amount of cinnamaldehyde remained at 0 day = (10.02/10.02)x100

= 100%

- *Cinnamaldehyde from hydrolysis of nanoparticles suspension at 16 day*

From equation (3) Y = 0.243X - 0.022

0.36 = 0.243X - 0.022

X = 1.57

Dilution factor = 333

X = 1.57 x 333

X = 523 ppm

Weight of cinnamaldehyde in 15 mL = 523 x 0.015

= 7.85 mg

∴ Relative amount of cinnamaldehyde remained at 16 day = (7.85/10.02)x100

= 78.30%

- *Cinnamaldehyde from hydrolysis of free aldehyde solution at 0 day*

From equation (3) Y = 0.243X - 0.022

0.476 = 0.243X - 0.022

X = 2.05

Dilution factor = 333

X = 2.05 x 333

X = 683 ppm

Weight of cinnamaldehyde in 15 mL = 683 x 0.015

= 10.25 mg

∴ Relative amount of cinnamaldehyde remained at 0 day = (10.25/10.25)x100

= 100%

- *Cinnamaldehyde from hydrolysis of free aldehyde solution at 16 day*

From equation (3) Y = 0.243X - 0.022

0.144 = 0.243X - 0.022

X = 0.68

Dilution factor = 333

X = 0.68 x 333

X = 226 ppm

Weight of cinnamaldehyde in 15 mL = 226 x 0.015

= 3.40 mg

∴ Relative amount of cinnamaldehyde remained at 16 day = (3.40/10.02)x100

= 33.90%

3.3 The amount of remained citronellal

- *Citronellal from hydrolysis of nanoparticles suspension at 0 day*

From equation (4) Y = 0.001X - 0.003

0.60 = 0.001X - 0.003

X = 603

Weight of citronellal in 15 mL = 603 x 0.015

= 9.045 mg

∴ Relative amount of citronellal remained at 0 day = (9.045/9.045)x100

= 100%

- *Citronellal from hydrolysis of nanoparticles suspension at 16 day*

From equation (4) Y = 0.001X - 0.003

0.419 = 0.001X - 0.003

X = 422

Weight of citronellal in 15 mL = 422 x 0.015

= 6.33 mg

∴ Relative amount of citronellal remained at 16 day = (6.33/9.045)x100

= 70.00%

- *Citronellal from hydrolysis of free aldehyde solution at 0 day*

From equation (4) Y = 0.001X - 0.003

0.897 = 0.001X - 0.003

X = 900

Weight of citronellal in 15 mL = 900 x 0.015

= 13.50 mg

∴ Relative amount of citronellal remained at 0 day = (13.50/13.50)x100

= 100%

- *Citronellal from hydrolysis of free aldehyde solution at 16 day*

From equation (4) Y = 0.001X - 0.003

0.241 = 0.001X - 0.003

X = 244

Weight of citronellal in 15 mL = 244 x 0.015

= 3.66 mg

∴ Relative amount of citronellal remained at 16 day = (3.66/13.50)x100

= 27.10%

3.4 The amount of remained citral

- *Citral from hydrolysis of nanoparticles suspension at 0 day*

From equation (5) Y = 0.109X - 0.003

0.634 = 0.109X - 0.003

X = 5.84

Dilution factor = 100

X = 5.84 x 100

X = 584 ppm

Weight of citral in 15 mL = 584 x 0.015

= 8.76 mg

∴ Relative amount of citral remained at 0 day = (8.76/8.76)x100

= 100%

- *Citral from hydrolysis of nanoparticles suspension at 16 day*

From equation (5) Y = 0.109X - 0.003

0.239 = 0.109X - 0.003

X = 2.22

Dilution factor = 100

X = 2.22 x 100

X = 222 ppm

Weight of citral in 15 mL = 222 x 0.015

= 3.33 mg

∴ Relative amount of citral remained at 0 day = (3.33/8.76)x100

= 38.00%

- *Citral from hydrolysis of free aldehyde solution at 0 day*

From equation (5) Y = 0.109X - 0.003

0.826 = 0.109X - 0.003

X = 7.61

Dilution factor = 100

X = 7.61 x 100

X = 761 ppm

Weight of citral in 15 mL = 761 x 0.015

= 11.42 mg

∴ Relative amount of citral remained at 0 day = (11.42/11.42)x100

= 100%

- *Citral from hydrolysis of free aldehyde solution at 16 day*

From equation (5) Y = 0.109X - 0.003

0.054 = 0.109X - 0.003

X = 0.52

Dilution factor = 100

X = 0.52 x 100

X = 52 ppm

Weight of citral in 15 mL = 52 x 0.015

= 0.78 mg

∴ Relative amount of citral remained at 16 day = (0.78/11.42)x100

= 6.80%

VITAE

Mr. Thapakorn Tree-udom was born on April 25, 1986 in Bankok, Thailand. He received a Bachelor's Degree of Science in Chemistry from Kasetsart University in 2007. And then, he started his graduate study a Master's degree in the Program of Petrochemistry and Polymer Science, Faculty of Science, Chulalongkorn University. During the undergraduate and master study, he had received a scholarship from the Development and Promotion of Science and Technology Talents project (DPST). During master study, he had a great opportunity to presented his work in poster session in the topic of "Fragranced chitosan nanoparticles: Schiff base formation and self-assembling" at the 7th International Symposium on Advanced Materials in Asia-Pacific (7th ISAMAP). The finance for joining the conference was supported by National Center of Excellence for Petroleum, Petrochemicals and Advanced Materials (NCE-PPAM) and the Graduate School, Chulalongkorn University.

His present address is 49/571 Krokkham, Muang, Samutsakhon Thailand 74000.